CHALMERS

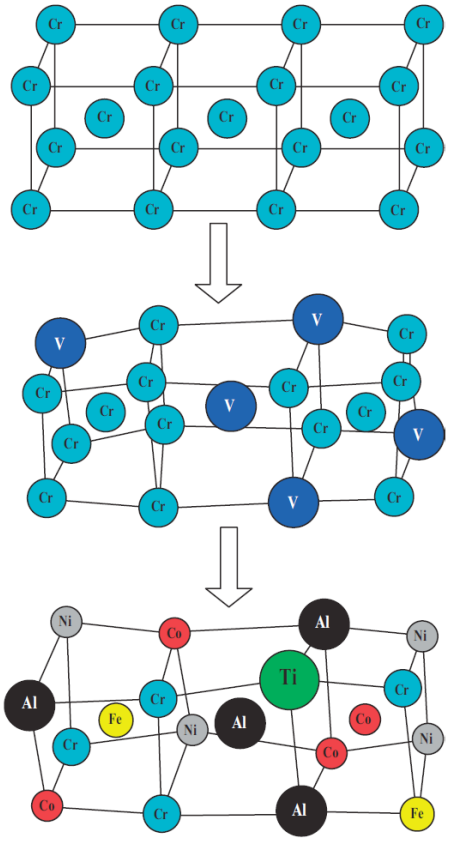

High Entropy Alloys: Breakthrough Materials for Aero Engine Applications?

Diploma work in the Master programme Applied Physics

DANIEL O. SVENSSON

Department of Materials and Manufacturing Technology
CHALMERS UNIVERSITY OF TECHNOLOGY
Gothenburg, Sweden 2015
Diploma work 2014

High Entropy Alloys: Breakthrough Materials for Aero Engine Applications?

by

DANIEL O. SVENSSON

Diploma work 2014
at Department of Materials and Manufacturing Technology
CHALMERS UNIVERSITY OF TECHNOLOGY
Gothenburg, Sweden

Diploma work in the Master programme Applied Physics

Performed at: GKN Aerospace Sweden AB
Flygmotorvägen 1, 461 38 Trollhättan

Supervisor: Ph.D., Adj. Associate Professor Magnus Hörnqvist
GKN Aerospace Sweden AB
Flygmotorvägen 1, 461 38 Trollhättan

Examiner and supervisor: Assistant Professor Sheng Guo
Department of Materials and Manufacturing Technology
Chalmers University of Technology, SE - 412 96 Gothenburg

High Entropy Alloys: Breakthrough Materials for Aero Engine Applications?

DANIEL O. SVENSSON

Diploma work 2014
Department of Materials and Manufacturing Technology
Chalmers University of Technology
SE-412 96 Gothenburg
Sweden
Telephone + 46 (0)31-772 1000

Cover:
[Schematic illustration of BCC crystal structure: (top) perfect lattice (take Cr as example); (middle) distorted lattice caused by additional one component with different atomic radius (take Cr-V solid solution as example); (bottom) serious distorted lattice caused by many kinds of different-sized atoms randomly distributed in the crystal lattice with the same probability to occupy the lattice sites in multi-component solid solutions (take AlCoCrFeNiTi0.5 as example) [1].]

Gothenburg, Sweden 2015

High Entropy Alloys: Breakthrough Materials for Aero Engine Applications?

DANIEL O. SVENSSON
Department of Materials and Manufacturing Technology
Chalmers University of Technology

SUMMARY
In this project the current literature regarding a relatively new materials type, high-entropy alloys (HEAs), was reviewed to find if they are applicable to aero engines, and in particular the engine parts made by GKN Aero Engine Systems in Trollhättan. To manage this the current state-of-the-art of aero engine materials was reviewed as well, partly via a literature survey and partly via discussions with company specialists at GKN Aero Engine Systems in Trollhättan. Based on these two reviews, several issues requiring further studies for future researchers to fill in the gap was identified, with possible solutions suggested where possible, and finally possible HEA systems were suggested for use in the specific engine parts manufactured by GKN Aero Engine Systems.

Keywords: High-entropy alloys, high entropy effect, aeropropulsion, high temperature structural materials.

Acknowledgements

The author wishes to thank Magnus Hörnqvist and Sheng Guo at Chalmers University of Technology for their help and supervision during this project. Aside from these, the help from Anders Hellgren, and Bengt Pettersson, GKN Aerospace Engine Systems Sweden regarding the properties of specific parts is greatly appreciated.

Daniel Svensson, Gothenburg 2015-01-09

Acronym/Symbol	Meaning
δ	Atomic Size Difference
κ	Thermal Conductivity
ρ	Density
A	Atomic Weight
CTE	Coefficient of Thermal Expansion
E	Modulus of Elasticity
G	Gibbs Free Energy
H	Enthalpy
S	Entropy
T	Temperature
T_m	Melting Temperature
VEC	Valence Electron Concentration
X	Atomic Fraction
AM	Additive Manufacturing
CMC	Ceramic Matrix Composite
HCF	High Cycle Fatigue
HEA	High-Entropy Alloy
HPC	High Pressure Compressor
HPT	High Pressure Turbine
HV	Vickers Hardness
LCF	Low Cycle Fatigue
LCS	Load Carrying Structure
LPC	Low Pressure Compressor
LPT	Low Pressure Turbine
MA	Mechanical Alloying
MTF	Mid Turbine Frame
PM	Powder Metallurgy
TBC	Thermal Barrier Coating
TBH	Tail Bearing Housing (see also TEC, TRF)
TEC	Turbine Exhaust Case (see also TBH, TRF)
TRF	Turbine Rear Frame (see also TBH, TEC)
UTS	Ultimate Tensile Strength
YS	Yield Strength

Contents

1

Introduction

The aero engine industry is ever changing, with new materials and techniques being developed continuously to be able to meet both the demands of passengers and government regulations. The engines produce less and less noice and use less and less fuel, reducing emissions more and more. One of the more effective ways to reduce fuel consumption is to lower the total weight of the engine, for instance by replacing the current materials with lighter ones. Other possibilities is to raise the working temperature of the engine (increasing the demands on the materials in the engine) or improving the design of the engine itself, turbines, compressors, fans etc.

At GKN Aerospace Engine Systems in Trollhättan, several engine parts for different aero (jet) engines are manufactured, some of which GKN has the design responsibility for and some of which are just manufactured at GKN according to instructions. For the parts which they have the design responsibility for they are always looking for possible improvements, and here the so called *high-entropy alloys* (HEAs) are very interesting. At the moment mainly due to their potential for lower densities than conventional high-temperature alloys (such as the currently used superalloys) as well as their generally good properties at elevated temperatures, with good softening resistance.

HEAs are alloys consisting of between five and thirteen principal components (components with a larger concentration), as opposed to conventional alloys which have at most three principal components. This gives rise to many promising properties, based mostly on what is known as the four core effects. These core effects are a *high entropy of mixing*, a *slower diffusion* than in conventional alloy systems, an increased *lattice strain* (due to the many differently sized elements) and finally a *cocktail effect*, leading to properties that at first may seem unintuitive. These effects and the properties they lead to will be discussed more in the following chapters.

This thesis is done together with GKN Aerospace Engine Systems in Trollhättan, and its purpose is to review what is known about HEAs today and, if possible, to suggest potential usages in aero engines, including both specific aero engine parts and promising

HEA systems. The aim is also to review the current status of materials in jet engines, which is covered in Chapter 2, while Chapter 3 will contain a review to some relevant developments in HEAs. These two reviews will be followed by Chapter 4, describing what is missing for HEAs to be able to work in jet engines, and finally Chapter 5, summarizing HEAs and their potential usage in aero engines.

2

State-of-the-Art of Aero Engine Materials

Today's aero engines are composed of different materials, Figure 2.1 shows a typical material distribution for a jet engine, and as can be seen it consists mostly of nickel alloys and titanium alloys along with some steels and aluminium alloys. The choice of alloys for different parts is heavily dependent on the working temperature and mechanical demands of the specific part along with the density of the alloy. An ideal alloy would be able to handle extreme temperatures while weighing next to nothing. This chapter will first give a simple description of how a jet engine works, followed by an introduction to the current materials in today's jet engines, with a brief description of aluminium alloys and steels and a more detailed description of titanium alloys and nickel alloys, since these are the alloys which are most commonly used in aero engines. A short introduction to some other new and promising types of material will also be given, including composites, ceramics and intermetallics. This will be followed by a description of the relevant specific parts in the aero engine, and the demands on these parts.

2.1 The Jet Engine

The jet engine basically works in four simple steps, *suck*, *squeeze*, *bang* and *blow*. During the suck stage air from outside of the engine enters at great volumes. The air is then squeezed together and mixed with fuel, and, following this, the fuel/compressed air mix is ignited at a constant pressure (bang), forcing the gas to expand through a turbine which then powers the compressor responsible for squeezing the air and then continuing further out of the engine (blow). It is normal to use between one and three compressors (often two), driven by separate turbines. According to Newton's third law "when one body exerts a force on a second body, the second body simultaneously exerts

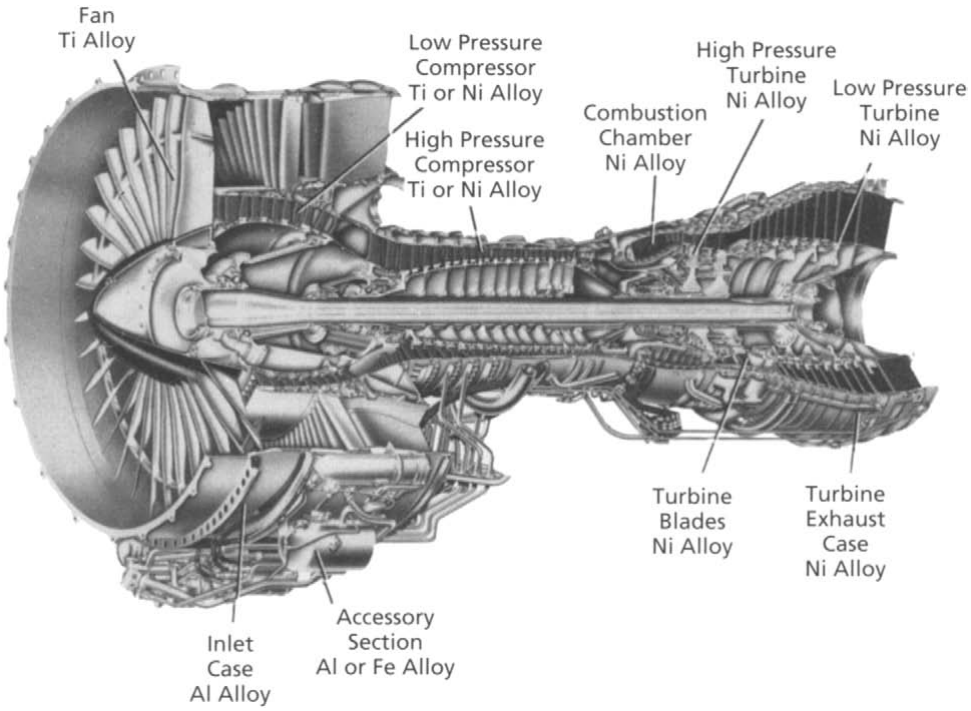

Figure 2.1: Typical material distribution of a jet engine [2].

a force equal in magnitude and opposite in direction on the first body", and with these great magnitudes of air molecules forced "backwards" at high speed a forward thrust for the engine is generated.

In military versions of the jet engine there is often an afterburner after the turbine exhaust where additional fuel may be injected and the stream again ignited. A more common version of the jet engine for civilian use is the *turbofan* jet engine, where at the front there is a large fan driven by one turbine which draws in and compresses air, partly into the core engine going through the stages outlined previously, and partly bypassing the core engine, contributing directly to the thrust. This is the type of engine seen in Figure 2.1. The version without the fan is called a *turbojet*.

That this procedure leads to elevated temperatures is easy to understand. First there is a rise in temperature when the air is compressed, the more compressed the higher the temperature, and with ignition this temperature is then again increased putting great demands on the combustion chamber and all parts downstream, especially so on the combustion chamber and the first turbine, but as work is extracted it is cooled down a bit to the next turbine.

2.2 Materials in Jet Engines

With different parts in the jet engine having different demands and limiting properties, many different materials are in use, though most of them stem from four major families, and these are *aluminium alloys*, *steels*, *titanium alloys* and *nickel alloys*. Outside of these four major material types there is also research and development being done on newer material types such as *ceramics*, *composites* and *intermetallics*. Each of these types of material will be described in this section, with the major focus on Ti-alloys and Ni-alloys, the most common materials in the jet engine today.

2.2.1 Aluminium Alloys

Aluminium alloys have among the lowest densities of the alloys in use in aero engines, with pure aluminium having a density of $2.7\,\mathrm{g/cm^3}$ [3]. They also show excellent fabricability and corrosion resistance [4]. Unfortunately, at elevated temperatures they loose some of their strength properties. The temperature limits are $\approx$ 200 - 250° C for a short time or $\approx$ 120 - 150° C for long-term usage [4], which is nothing compared to the $\approx 1500\,^{\circ}\mathrm{C}$ which may be reached in, as well as downstream of, the combustion chamber in a jet engine [5]. It also has a lower modulus of elasticity than for instance steels and titanium alloys (69 GPa versus 200 GPa and 110 GPa [3], respectivley). Typical alloys used in jet engines are 2xxx, 6xxx and 7xxx-series wrought alloys and 3xx-series cast alloys.

2.2.2 Steels

The main advantage of steels is often their price, steels being based on iron and carbon which are two of the cheapest elements. Steels typically used in jet engines are: low alloy high strength steels (in shafts and gears bearings), austenitic stainless steels (in tubings) as well as martensitic and precipitation hardening steels (in frames and casings).

2.2.3 Titanium Alloys

Titanium alloys have a high strength-to-weight ratio, good fatigue strength, better corrosion resistance than both aluminium and steel alloys and they can work at higher temperatures than aluminium alloys (up to 600°C) [6, 7, 8]. Titanium exists in two different crystalline forms, the hexagonal close packed (hcp) α phase, which is stable at lower temperatures, and the body-centered cubic (bcc) β phase which is stable at elevated temperatures, from $\approx$ 880° C to the melting point. This solvus temperature can be changed with alloying elements, giving great configurability of the properties of titanium alloys.

Titanium alloys (some of which can be seen with some basic mechanical properties given in Table 2.1) are divided into four classes depending on the ratio of α and β phases at room temperature. The classes are 1) α and 2) *near* α, which consists of

Table 2.1: Mechanical properties of some titanium alloys. [9]

Alloy	**Density** (g/cm^3)	**Yld.Str.** (MPa)	**Tens.Str.** (MPa)	**10^7Cyc. Fat. Str.** (MPa)
Commercially Pure	4.51	351	483	244
Ti-6%Al-4%V	4.42	911	999	609
Ti-4%Al-4%Mo-2%Sn-0.5%Si	4.60	1035	1136	626
Ti-10%V-2%Fe-3%Al	4.65	1228	1311	721
Ti-6%Al-2%Sn-4%Zr-2%Mo	4.54	917	1012	558

mostly the α phase, where the alloys usually have $\approx 5-6\%$ Al along with some Sn and Zr for solid solution strengthening as well as some β phase stabilizers. These alloys have good elevated temperature properties, with good creep resistance and strength retaining. There are also 3) α/β alloys, which have sizable portions of both α and β phases. These have the best balance of mechanical properties. The most common titanium alloy, Ti-6Al-4V, which accounts for about 60% of all produced titanium alloys [7], is this type of alloy. They have good room temperature properties and good elevated temperature properties for short amounts of time. The last class is 4) *metastable* β, which shows high deformability, but also high density and reduced ductility when heat treated to peak strength levels.

The properties of Ti alloys make them suitable for the cooler parts of the engine. It is commonly used in the fan disk, where the limiting properties are low cycle fatigue (LCF) and fatigue crack growth. Common alloys in this scenario are Ti-6Al-4V, Ti-5Al-2Zr-2Sn-4Cr-4Mo and Ti-6Al-2Sn-4Zr-6Mo. Another common area of use is in the compressor rotor (both low pressure compressor (LPC) and high pressure compressor (HPC) rotor), which can have up to seven stages, where the first stages often are limited by LCF and the last stages are limited by creep. The most common alloy for the front stages is Ti-6Al-4V and the most common for the back stages is Ti-6Al-2Sn-4Zr-2Mo+Si (for the HPC the final stages are exposed to temperatures too high for the titanium alloys and are instead made of nickel-based alloys). The fan blades and between six and eight stages of the compressor air foils are also ordinarily Ti alloys, most often Ti-6Al-4V. These are limited by high cycle fatigue (HCF), but also by their resistance to impact damage from foreign objects. Ideally higher-strength alloys would be used, but those are often too difficult to fabricate. There are also many static components made of titanium alloys such as frames, casings etc. [8] A problem however is their relatively low stiffness, as mentioned in section 2.2.1

Titanium alloys are also used in structural parts and casings in the cooler parts of the engine, for instance in the intermediate compressor casing (ICC), which consists mostly out of Ti-6Al-44 and Ti-6Al-2Sn-4Zr-2Mo.

2.2.4 Nickel-based Alloys

When the temperature is too high for titanium alloys ($\geq 550\,^{\circ}\mathrm{C}$), the most common replacement is the nickel-based *superalloys* (so named due to their superior properties compared to ordinary alloys). These alloys show high strength, good fatigue and creep resistance along with good corrosion resistance. They are also able to sustain these properties over extended periods of time at higher temperatures. Of the total engine weight about half is due to these superalloys [2, 8, 10]. Aside from the nickel based superalloys, there are also nickel-iron based and cobalt based superalloys, but since most of the superalloys in a jet engine is nickel-based or nickel/iron-based they will be the focus of this section.

Nickel-based superalloys have a face centered cubic (fcc) austenite γ matrix and get their strength from a combination of solid solution hardening, precipitation hardening with γ' and γ'' phases as well as a presence of carbides at the grain boundaries. Many different elements are added to the matrix to achieve the sought after properties of these materials, and the most common ones and their purpose can be seen in Table 2.2.

Table 2.2: Role of alloying elements in superalloys. [2, 11]

Alloy additions	Solid Solution Strengtheners	γ' Formers	Carbide Formers	Grain Boundary Strengtheners	Oxide Scale Formers
Chromium	x		x		x
Aluminium		x			x
Titanium		x	x		
Cobalt	x				
Molybdenum	x		x		
Tungsten	x		x		
Boron				x	
Zirconium				x	
Carbon				x	
Niobium		x	x		
Hafnium			x	x	
Tantalum		x	x	x	

The γ' formers are responsible for the precipitation hardening, especially so Al and to some extent Ti, which together with Ni form the fcc ordered $Ni_3(Al,Ti)$ γ' phase. This phase only has a 0.1% lattice mismatch with the γ matrix, giving it a long term stability, and a typical microstructure can be seen in Figure 2.2. There are also nickel alloys with other precipitate phases for strengthening, for instance adding niobium to nickel creates the γ'' Ni_3Nb precipitates which is one of the strengthening methods in

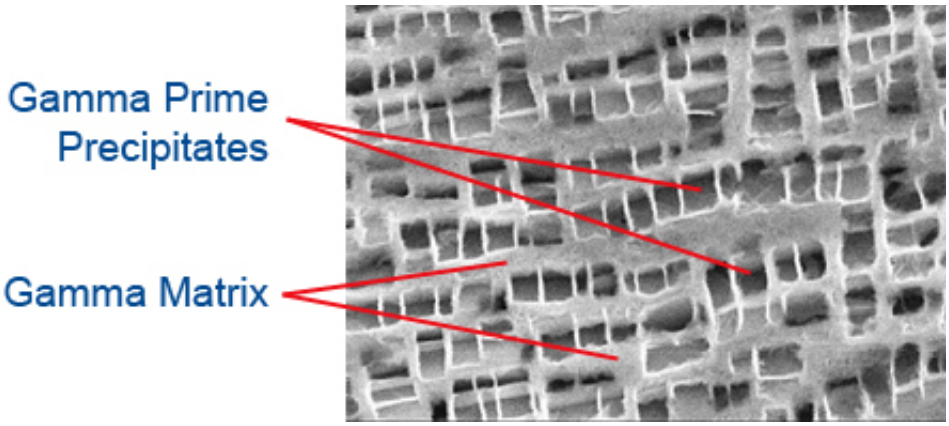

Figure 2.2: The γ matrix with γ' precipitates. [12]

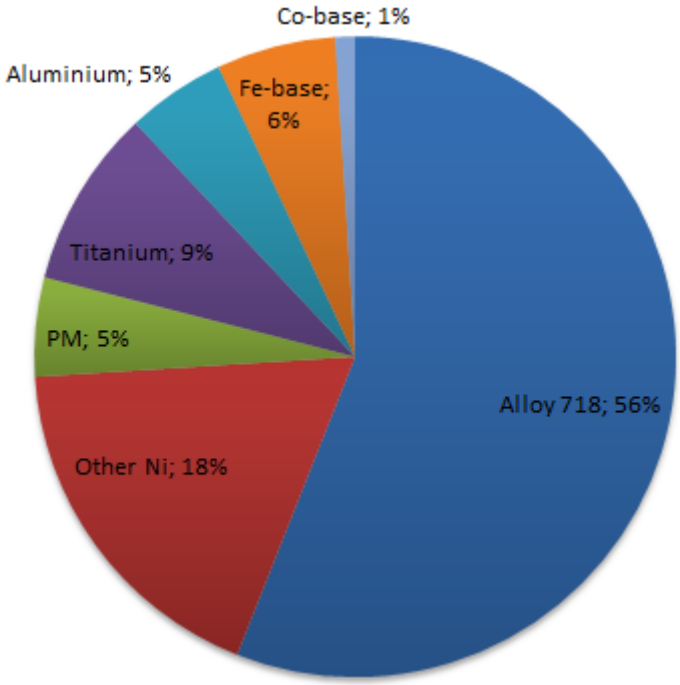

Figure 2.3: Material used in General Electric Aero Engines rotating and structural forgings for the year 2000 (all materials except those made by PM were made by casting). [13]

the nickel/iron alloy Inconel 718, which is by far the most used superalloy (Figure 2.3 shows the materials used by GE aviation in the year 2000, where Inconel 718 was the most used material).

As mentioned earlier the nickel based alloys are most often the material of choice in the hotter parts of the engines (this despite their relatively high density), such as the last stages of the HPC, the high pressure turbine (HPT) and the low pressure turbine

(LPT). Here LCF life and fatigue crack growth are limiting properties [2]. For the air foils in the HPT, oxidation resistance is also an important property for the material [8]. The turbine disks have often been made of Inconel 718 [14], but alloys manufactured via powder metallurgy (PM) processing has also been used with alloys like LC Astroloy[1] and Rene95[2] [14]. There are several reasons for choosing PM over conventional casting, including: it minimizes the segregation of elements making the alloys more homogeneous; some alloys cannot be forged by conventional methods; it can to a greater extent be made to certain shapes, reducing the need for machining and raw materials, along with other benefits.

For parts where creep resistance is of extreme importance, such as the turbine blades in the early part of the turbine, the parts may be cast as single crystals using alloys such as CMSX4[3], DMS4[4] and TMS196[5] (able to withstand temperatures up to $\approx 1140\,^{\circ}\mathrm{C}$ [14]), removing high-angle grain boundaries and thus removing creep arising from grain boundary sliding [8, 10]. This also removes the necessity for grain boundary strengthening elements in the alloy. Generally it has been that when creating new generations of single crystal superalloys with improved creep resistance the density has increased. This is attributed to the increase of refractory elements and decrease of chromium in the newer generations [15, 16]. New lower density single crystal superalloys is being researched however, with densities in the vicinity of $8.5\,\mathrm{g/cm^3}$ [15].

Since it is rather expensive to cast single crystals, parts where the creep resistance is not quite as important (but still important) such as in the blades of the later, somewhat colder parts of the HPT and in the LPT it may be enough with directionally solidified alloys (alloys cast with the grain boundaries in parallel with the direction of the load) such as PWA1422[6] and DMD4[7] [14] since these are cheaper [10]. Vanes, having to face long periods of time at elevated temperatures have often been made by oxide dispersion strengthened superalloys, such as MA754[8] [14].

2.2.5 Newer Material Types

Some newer material types currently being researched will be briefly described in this section, ceramics, intermetallics and composites (such as ceramic matrix composites).

Ceramics

The excellent heat resisting properties of ceramic materials such as Al_2O_3 and SiC make them interesting for the hotter parts of the engine. They are also lighter and cheaper than the superalloys relevant for the same parts (up to 40 % lighter and cost

[1] 56.5Ni15Cr15Co5.25Mo3.5Ti4.4Al0.06C0.03B0.06Zr
[2] 61Ni14Cr8Co3.5Mo3.5W3.5Nb2.5Ti3.5Al0.16C0.01B0.05Zr
[3] 61.7Ni6.5Cr9Co0.6Mo6W3Re6.5Ta0.1Hf1Ti5.6Al
[4] 67Ni2.4Cr4Co5.5W6.5Re9Ta0.1Hf0.3Nb5.2Al
[5] 59.7Ni4.6Cr5.6Co2.4Mo5.0W6.4Re5.6Ta0.1Hf5.6Al5.0Ru
[6] 59.2Ni9Cr10Co12W1.5Hf1Nb2Ti5Al0.1Zr0.14C0.015B
[7] 66.8Ni2.4Cr4Co5.5W6.5Re8Ta1.2Hf0.3Nb5.2Al0.07C0.01B
[8] 78Ni20Cr1Fe0.05C0.3Al0.5Ti0.6Y_2O_3

only 5 % of what superalloys do [14]). As will be mentioned in section 2.3, ceramics are often used as coatings for parts exposed to high temperatures. Manufacturing whole parts out of ceramics is not currently viable however, due to their brittleness, and today they are mostly used in coatings.

Composites

Several types of composites are interesting for the aerospace engine industry. There are several types of composites, for instance Ti-MMC, which has SiC fibers in a Ti-matrix. If the problem with properties degradation from fibre-matrix interaction in Ti-MMCs can be solved they are also very interesting for further aero engine usage, since they could be used in a bladed ring as opposed to the traditional disc and dovetail arrangement, reducing the weight by $\approx 70\%$. For colder sections polymer matrix composites such as epoxy resin-carbon fiber composites are currently being used, the aforementioned composite is for instance used by GE in its front fan blades, thus reducing their weight as compared with metal-based turbine blades. [14]

There is also ceramic matrix composites (CMCs), with their excellent fracture toughness [17] and possibility to withstand temperatures up to 1500 °C [18] along with their low densities, making them promising for usage in aero engines. The high temperature limit means that air cooling is not quite as necessary as it is with superalloys, meaning great design gains can be made. The most common CMCs use SiC-matrices, with varying fibers dependant on applications, often it is SiC-fibers or just carbon [14, 17, 18], but Al_2O_3/Al_2O_3 is also common. There are however still some issues with the durability, reliability, manufacturing, design and cost [14, 18], and CMCs have mostly been tried in non-rotating parts such as exhaust nozzles on military engines (where a weight saving of $\approx 50\%$ was gained [18]), afterburner components, combustion chambers and turbine nozzle vanes [14, 17, 18].

Intermetallics

Certain intermetallics have been of interest for aero engine usage. The most researched intermetallics are based on aluminium together with either titanium or nickel, with the most focus on γ TiAl and β NiAl. These alloys have a rather low density compared to the usual superalloys, mainly due to their large fractions of aluminium. The high aluminium content also leads to good oxidation properties. As intermetallics their ordered structure gives them a rather high melting point and they have comparatively good creep properties, however only in specific temperature intervals [14, 19]. They do have quite a lot of drawbacks however, including (but not limited to) the high sensitivity of the properties on the composition (since the intermetallic phase needs to form), a certain brittleness at temperatures below 650 °C for γ TiAl and 1000 °C for β NiAl [19]. The brittleness also leads to poor manufacturing properties [19].

So far, even though it should be rather fitting for turbine parts exposed to temperatures of $1100 - 1600$ °C, the β NiAl is not used anywhere, mostly due to the aforementioned poor manufacturability properties and its brittleness [19]. γ TiAl has had a bit

more research and development done, and currently we are in the third generation of γ TiAl based alloys, which are able to withstand temperatures from room temperature up to 850 °C, making LP compressor components a possible application. The second generation γ TiAl alloys have a temperature range of $650 - 750$ °C and since they also have good HCF properties they are interesting for blades and shrouds of the HP compressor, where a possible weight saving of 20% was expected [19]. There was in fact successful demonstration programs for among other parts LPT turbine blades as well as HP compressor blades and shrouds [19].

There are still however rather large problems with these materials, with for instance a large scattering in mechanical properties, a low tolerance to defects, comparatively high production costs and manufacturing difficulties [14, 19]. These problems are not final though, and for instance GE is using γ TiAl for LPT blades in their engines [20]. As a curiosity when talking about the development of new materials it can be said that the research and development costs for GE regarding γ TiAl is calculated to $\approx$ \$40 million, with additional costs of $>$ \$85 million to industrialize it for turbine blades [21].

2.3 Coatings in Jet Engines

Another way to make the materials able to withstand the different environments is to coat them with a protective layer. There are basically three types of coatings today, one type of which are *aluminide coatings* (also known as diffusion coatings) which are meant to protect against oxidation by creating an aluminide layer (CoAl or β-NiAl) by letting aluminium react with the nickel or cobalt in the base metal. There are also *overlay coatings*, which are coatings where all of the elements comes from the coating itself, with no elements coming from the substrate, and here the thickness is not as dependant on processing conditions. Overlay coatings are most often of the form MCrAlY, where M is either iron, nickel, cobalt or a combination. These often have improved corrosion resistance, much due to the effect of yttrium. WC-Co is another type of coating, which is used mostly at parts susceptible to wear due to the high hardness of the coating.

Third, we have *thermal barrier coatings* (TBC), which as the name suggests are used to make the substrate materials able to operate at higher temperatures than they normally do, and they can lower the surface temperature of the relevant superalloys by $100 - 200$ °C [5, 22]. TBCs are most often based on the ceramic Y_2O_3-stabilized ZrO_2, which has a very low thermal conductivity at elevated temperatures (≈ 2.3 W/mK at 1000 °C [22]) and a high coefficient of thermal expansion ($11{\cdot}10^{-6}$ °C^{-1} [22]) allowing it to alleviate stresses from the mismatch between the ceramic and the underlying metal. The so-called *misfit strain* arising from differences in thermal expansion is one of the limiting properties durability-wise during the thermal cycles and must therefore be managed [23]. Sought after properties of TBCs are low thermal conductivity and stability during the thermal cycles along with resistance to erosion and pollutants [5]. There are several factors contributing to the thermal conductivity of coatings: the density of the coating, the number of internal boundaries and pores. These along with the orientation of the internal cracks and pores relative to the thermal flux are the major contributors and will

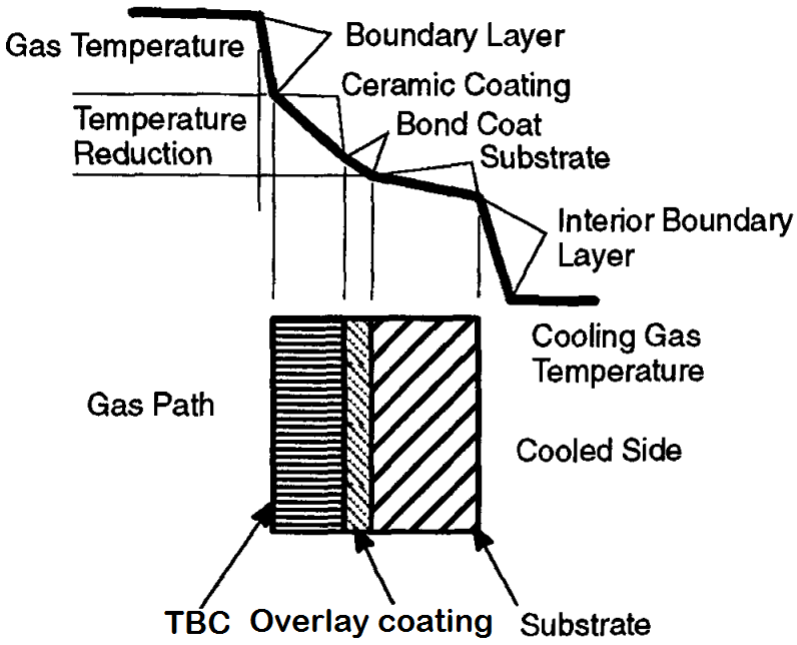

Figure 2.4: Schematic of a TBC on an air-cooled gas turbine engine component. [24]

have to be controlled for as effective TBCs as possible [5].

TBCs are applied above an overlay coating of MCrAlY or on an aluminide coating which is for the oxidation resistance along with providing a rough enough surface for the TBC to bond to. Figure 2.4 gives a description of the different layers in a TBC. TBCs are often used in applications like nozzle guide vanes and blade platforms [14]. If one were to find a TBC with among other things a coefficient of thermal expansion that matches that of the substrate material, it would not only be a shielding coating but also a load bearing one, giving another use to the coating.

2.4 Specific Parts

Choosing the specific parts which at first will be relevant for HEAs two major factors was identified. Firstly, that HEAs shows great potential for relatively low densities. Perhaps not lower than titanium alloys but still lower than nickel based superalloys. Secondly, they show great promise for high temperature stability. These properties (which will be discussed more in Chapter 3) indicate that HEAs could be potential replacement materials for the hotter structural components downstream of the combustion chamber, such as the turbine exhaust case and the mid turbine frame, but also the turbine exit (nozzle and cone) as these parts today are composed mainly out of the relatively heavy nickel alloys, while the cold structural parts are made out of lighter elements such as

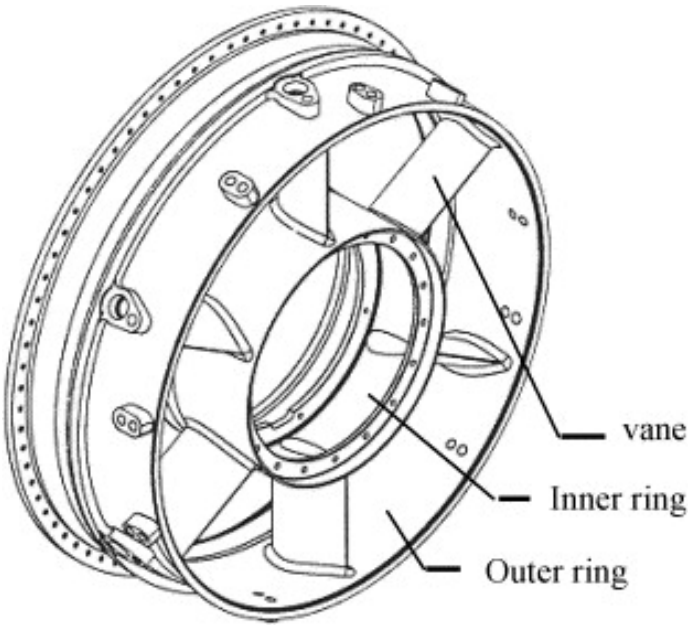

Figure 2.5: Simple sketch of a TEC. [25]

titanium alloys. These hot structural parts will therefore be described in more detail in this section.

2.4.1 Turbine Exhaust Case

After (downstream of) the final turbine in the jet engine one finds the turbine exhaust case, also known as the turbine rear frame or the tail bearing housing. The purpose of this part is to support the end of the LP rotor, mount the engine to the aircraft body as well as to remove the angular component of the outgoing flow. Figure 2.5 shows the main components of the TEC, the inner and outer rings as well as the vanes.

While the temperatures of the gas in the TEC is not quite as high as in the turbines due to work being extracted from the gas it still have to face rather high temperatures and it thus must be able to retain some of its mechanical properties to continue its function as engine mount. It also need to be corrosion and oxidation resistant at these elevated temperatures, while being weldable, formable and generally malleable. Unfortunately it is not sufficient to just have these properties. The materials used in the TEC must also be fatigue resistant (primarily LCF), not too heavy, weldable, malleable, and generally able to shape and join. Today Inconel 718 is the most used alloy in the TEC, being able to face temperatures of $\approx 650\,^{\circ}\mathrm{C}$.

Another reason for the importance of weldability, other than for the joining of different parts, is that it is related to and opens up the door (or rather keeps the door open) for additive manufacturing (a form of 3D-printing). This is a technique that in the future could be a material saver, for instance when having extending parts on a circular disk

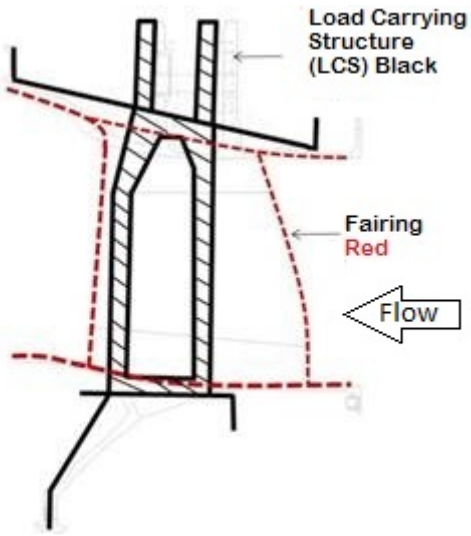

Figure 2.6: Sketch of separation of functionality in TEC and MTF, with supporting material (LCS) inside heat shielding fairings in the flow path.

these parts can be added layer by layer. This instead of starting from a disk of a wider diameter and then machining away the unwanted material which leads to quite a waste of materials.

One possible change in the layout of the TEC is to separate the functionality of the vanes, with a supporting structure inside heat shield fairings made of some solution hardened alloy (see Figure 2.6 for a simple sketch). The heat shield materials are preferably solution hardened since these types of alloys does not loose their properties as easily as precipitation hardened alloys at increased temperatures and since they are easy to process. The limiting properties for the load carrying structure (LCS) inside the fairings is primarily *LCF* properties, followed by *strength*, *stiffness*, *creep/thermo mechanical fatigue* and *oxidation properties*, and the primary alloy for this is today Inconel 718. Also, with LCSs, an elongation at fracture of at least 5% is wanted. The materials for heat shielding fairings are limited primarily by their *temperature capability* (e.g. thermal stability, creep deformation), followed by their *formability* and *oxidation* properties. The working temperatures for the heat shields are expected to be $\approx 670\,^{\circ}\mathrm{C}$ with peak temperatures of $\approx 760\,^{\circ}\mathrm{C}$. It is expected though that in the future these temperatures may reach as high as $\approx 900\,^{\circ}\mathrm{C}$ with average temperatures of $\approx 800\,^{\circ}\mathrm{C}$.

The composition of some typical precipitation hardened and solution hardened alloys can be seen in Table 2.3, and some describing parameters for the aforementioned properties and typical alloys can be seen in Table 2.4.

2.4.2 Mid Turbine Frame

Upstream of the TEC in the engine, between the high pressure and low pressure turbines, is the mid turbine frame (MTF), which can be seen in Figure 2.7. This houses

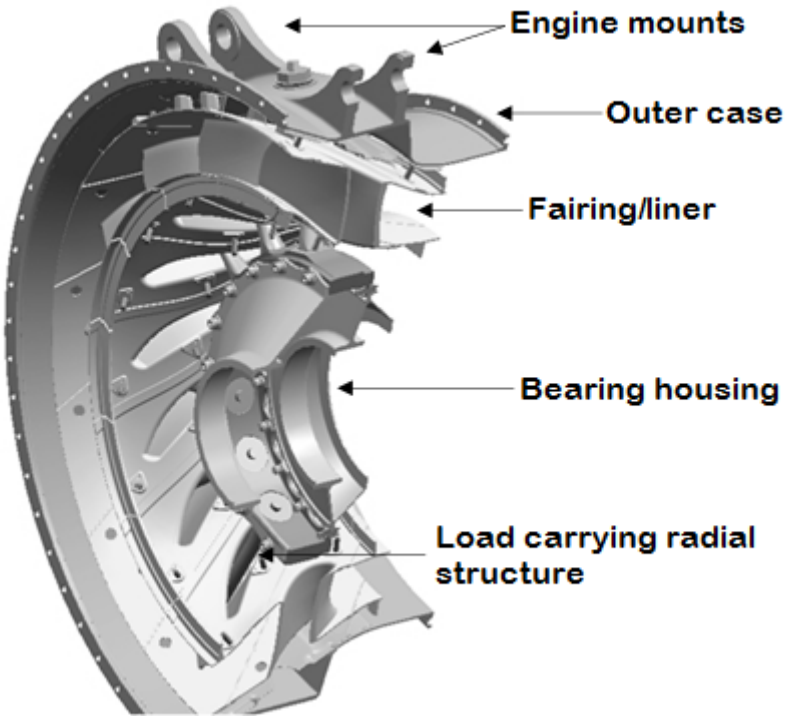

Figure 2.7: Model of a generic MTF.

the mid turbine bearing supporting the HP and LP rotors and transmits their loads to the outer casing. The demands on the MTF are somewhat similar to the demands on the TEC, but since the MTF is situated before the low pressure turbine the temperature of the gas is a bit higher. It needs to have a certain stiffness to make sure that the blade tips are able to rotate without being hindered by the casings, something which must be true during both normal flight and more extreme maneuvers. The MTF is today mostly made out of nickel alloys, which is due to the aforementioned high temperatures.

The MTF normally has a separation of functionalities as described in the previous section, with vanes composed of a LCS protected by a heat shielding fairing. The limiting properties for the LCS are similar to those of the LCS for the TEC, with primarily *LCF* properties, followed by *strength* and *stiffness* properties. The most interesting alloy for this today is again Inconel 718. The alloy choice for the fairings is limited primarily by their *creep strength* properties, followed by their *oxidation* properties and *LCF/thermo mechanical fatigue*. The alloys looked at in the present is the Ni-based Mar-M-247 and the Co-based Mar-M-509.

2.4.3 Nozzle and Exhaust Cone

Downstream of the TEC we find the final parts of the (civilian) jet engine, the nozzle and exhaust cone (in jet engines for military applications there is often also an

Figure 2.8: Picture of an exhaust cone and nozzle attached to an aeroplane. © Boeing

afterburner), seen in Figure 2.8. The existing cones of today are most often made out of a titanium alloy, but cones for newer engines are made out of solution hardened superalloys. The research for future cones today is mostly focused on CMC based on Al_2O_3 and SiC. Limiting properties are among others *creep properties*, *temperature capability*, *surface stability* and *weight* (density). If the nozzle and cone could be manufactured together with the TEC instead of separately, care could be taken to improve the properties of the interfaces that arise when the three separate parts are assembled together.

Table 2.3: Composition in weight % for the superalloys Inconel 718 [26], Waspaloy [27] and Haynes 230 [28]. * denotes that the element is used for balance, ' denotes that it is the maximum allowed value.

Alloy	Ni	Co	Cr	W	Mo	Fe	Mn	Si	Al	C	La	B	Ti	Cu	Zr	Nb+Ta
Inconel 718	50-55		17-21	-	2.8-3.3	*	-	-	0.2-0.8	-	-	-	0.65-1.15	-	-	4.75-5.5
Waspaloy	58*	13.5	19	-	4.3	2'	0.1'	0.15'	1.5	0.08	-	0.006	3	0.1*	0.05	-
Haynes 230	57*	5'	22	14	2	3'	0.5	0.4	0.3	0.1	0.02	0.015'	-	-	-	-

Table 2.4: Key values for some properties for the precipitation hardened conventional alloy Inconel 718 (1/2 inch bar stock), solution hardened Haynes 230 (sheet) and precipitation hardened Waspaloy (sheet)

Property	**Inconel 718**	**Haynes 230**	**Waspaloy**
Density (g/cm^3)	8.19 [29]	8.97 [28]	8.20 [27]
UTS (RT) (MPa)	1375 [29]	860 [28]	1335 [27]
UTS (650°C) (MPa)	1100 [29]	670 [28]	1195 [27]
$\sigma_{0.2}$ (RT) (MPa)	1100 [29]	390 [28]	910 [27]
$\sigma_{0.2}$ (650°C) (MPa)	980 [29]	270 [28]	770 [27]
$\sigma_{0.2}$ (RT, after 650°C exposure for 1000 h) (MPa)	-	440 [28]	-
ϵ (650°C) (%)	25 [29]	55.3 [28]	20.8 [27]
Modulus of elasticity (RT) (GPa)	208 [30]	211 [28]	213 [27]
CTE (RT) ($\cdot 10^{-6}\,K^{-1}$)	13.0 [29]	12.7 [28]	13.9 [27]
CTE (650°C)($\cdot 10^{-6}\,K^{-1}$)	15.1 [29]	15 [28]	14.8 [27]
Thermal conductivity (RT) ($W/m \cdot K$)	11.4 [29]	8.9 [28]	-
Thermal conductivity (650°C) ($W/m \cdot K$)	-	21.4 [28]	20 [27]
Stress for rupture after 1000h at 650°C (MPa)	896 [30]	295 [28]	550 [27]

3

High-Entropy Alloys

High-entropy alloys (HEAs) is a rather novel subject with many possible applications. Even though the concept dates back to the 70s with the work of Cantor et. al. [31] (or even the late 18th century with studies by Franz Karl Achard [31]) it was not until 2004 that it really took foot with the discoveries by Yeh et al. [32]. This opened up a new world for materials scientists and a lot of research has been done since then. This chapter is aiming to review the current status of HEAs, with focus on properties relevant for use in aerospace engines. This includes among others, strength, fatigue, wear and high temperature properties. It will begin with the definition of HEAs along with typical properties and processing routes. This will be followed by a closer look at why they are potential materials for use in aerospace engines.

3.1 Introduction to HEAs

This introduction will contain the definition of HEAs. There will also be some discussions regarding different phases in HEAs along with how they may be predicted.

3.1.1 Definition

A rather simple definition of HEAs is to consider alloys of five or more metallic elements where each of these elements has a concentration of between 5 and 35% as HEAs [32]. There can also be elements with a lower concentration than 5%, and these are called *minor* elements, as opposed to *principal* for those in higher ratio. This was the definition given by Yeh et al. in 2004 [32].

There are however other definitions, and even though the scope of materials is very similar there are some differences. One main definition is to go by the configurational entropy of the alloy, and this was proposed by Miracle et al. [33]. This is due to that one of the major effects of HEAs is their high entropy of mixing ΔS_{mix}, of which the

configurational entropy ΔS_{conf} is a major part. Before going into the definition, the reasoning for the name *high-entropy* alloys will be given.

Historically, alloys have consisted of between one and three principal element(s) and then one or more minor elements, added in small concentrations to change the properties of the principal element(s). For instance *steel*, which is based on the principal element iron with the addition one or more minor elements such as carbon, or the more complicated superalloys discussed in the previous chapter. This is rather severely limited by the number of existing elements in the periodic table when it comes to the number of possible systems. Even though the possibility to add more principal elements into the mix always has existed, there has also been a fear, based on metallurgical knowledge gained from among other things phase diagrams for ternary alloys, that this would lead to alloys consisting of several co-existing phases, consisting of among others ordered phases, both complex intermetallics (intermetallic compounds such as Laves phases) and the more simple ordered fcc,bcc,hcp-derivations. This high amount of phases would make these multi-principal component alloys very hard to control.

Surprisingly then, when multi-principal alloys were finally tried, there were mostly disordered solid solutions, with less compound formation than expected [32]. This is attributed to the aforementioned high entropy of mixing. It is known that the equilibrium phase of a system is decided by which phase has the lowest Gibbs free energy,

$$\Delta G_{\text{mix}} = \Delta H_{\text{mix}} - T\Delta S_{\text{mix}}, \tag{3.1}$$

where H is the enthalpy, T is the temperature and S is the entropy. From the entropy part in equation (3.1) we can see that the disordered phases with a high configurational entropy will gain an advantage over the ordered phases with a lower entropy. This will help suppress some of the ordered phases (promoted by their negative enthalpies of mixing), and especially so at higher temperatures.

The configurational entropy per mole for an ideal disordered solution is given by

$$\Delta S_{\text{conf}} = -R\sum_{i}^{n} X_i \ln(X_i) \tag{3.2}$$

where R is the gas constant ($= 8.314\,\text{J}\cdot(\text{mol}\cdot\text{K})^{-1}$), X_i is the atom fraction of the ith element and n is the total number of different elements. An ideal solution is a valid approximation for liquids as well as for solids near their melting temperatures. For an equimolar alloy (where all elements have the same concentration) with n different components that means that there is a configurational entropy of $S = R\ln(n)$, which equals to $1.61R$ when $n = 5$. Using this, Miracle et al. [33] has defined HEAs to be alloys with $\Delta S_{\text{conf}} \geq 1.5R$. This does not include all possible combinations from the earlier definition, according to which the minimum for a 5-element alloy is $\Delta S_{\text{conf}} = 1.36R$, when two components have the ratio 0.35, one has 0.20 and the final two has 0.05, but other than this they pretty much describe the same systems.

The $1.5R$ value is chosen since the lower bound for the 5-element alloy is lower than the equimolar ratio for the 4-element alloy. There are also some conventional alloys

with $\Delta S_{\text{conf}} \approx 1.36R$. It should also be mentioned that for the Miracle definition, there is some ambiguity since the phase changes with temperature, and one alloy that is a solid solution above a certain temperature may not be it below. They therefore made the decision to classify HEAs based on their high temperature configurational entropy. Using this method they also define low-entropy alloys as those with $\Delta S_{\text{conf}} \leq 1.0R$ and medium-entropy alloys as those with configurational entropy $1.0R < \Delta S_{\text{conf}} < 1.5R$.

A third definition has been suggested by Otto et al. [34], who suggested that only true solid solution forming multi-component alloys should be called high entropy alloys, since the multi-component alloys with intermetallic phases does not exhibit the "full" configurational entropy shown by the true solid solutions, as they are not completly disordered.

3.1.2 Phases in HEAs

Even though many complex phases are suppressed by the high configurational entropy they are still a possibility. Studies have been made regarding how to predict phase formation in different alloy systems. Starting from the Hume-Rothery rules for solid solutions in low-entropy alloys [35], which says that important parameters are among others atomic size difference, electron concentration, electronegativity, several parameters for prediction of the formation of solid solutions have been identified [1, 36]. These are the (earlier mentioned) enthalpy of mixing and configurational entropy, along with a parameter for the atomic size differences δ. The entropy is calculated using the formula for configurational entropy in equation (3.2), and the enthalpy is calculated according to $\Delta H_{\text{mix}} = \sum_{i=1, i\neq j}^{n} \omega_{ij} X_i X_j$, where $\omega_{ij} = 4\Delta H_{\text{AB}}^{\text{mix}}$ is the regular melt-interaction parameter between element i and j and $\Delta H_{\text{AB}}^{\text{mix}}$ is the mixing enthalpy of binary liquid alloys. Finally, the atomic size difference is calculated according to $\delta = 100\sqrt{\sum_{i=1}^{N} X_i(1 - r_i/\bar{r})^2}$ where the factor 100 is for numerical clarity, r_i is the atomic radius of element i and $\bar{r}$ is the (weighted) average atomic radius of all elements. Ren et al. [37] plotted ΔH_{mix} versus δ for some systems, and the result can be seen in Figure 3.1.

If one wants a solid solution these parameters should follow these conditions $-22 \leq \Delta H_{\text{mix}} \leq 7\,\text{kJ/mol}$, $\delta \leq 8.5$ and $11 \leq \Delta S_{\text{conf}} \leq 19.5\,\text{J} \cdot (\text{mol} \cdot \text{K})^{-1}$ [1, 36]. The general look of these conditions is quite reasonable, as noted by Tsai and Yeh [39]. Starting with the enthalpy a too large negative value would lead to intermetallic phases and a to large positive value would lead to phase separation. As for the atomic size difference, a too large difference would mean excess strain energy and would destabilize the simple structures. Finally, a large configurational entropy works as described in the previous section. These conditions may still give ordered phases, but most likely only the simple kind, the earlier mentioned derivations of fcc,bcc and hcp solid solutions, and not the complex intermetallics. The disordered phases have a bit more narrow conditions, with $-15 \leq \Delta H_{\text{mix}} \leq 5\,\text{kJ/mol}$, $\delta \leq 4.3$ and $12 \leq \Delta S_{\text{conf}} \leq 17.5\,\text{J} \cdot (\text{mol} \cdot \text{K})^{-1}$ [1, 39].

Talking about these parameters it is worth briefly mentioning bulk metallic glasses, which is also a type of material based on the concept of several constituting elements. The rules for the formation of these are however that there should be a large atomic

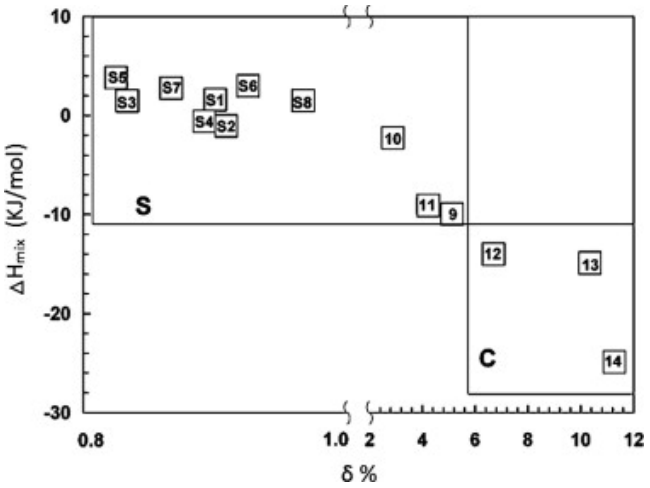

Figure 3.1: Relationship between δ and ΔH_{mix} in some HEAs. (S: indicates the alloy containing only solid solution; C: indicates the alloy containing intermetallics; S1–S8 from Ref. [37]; 9–14 from Ref. [38]). 9: CrFeCoNiAlCu0.25, 10: VCuFeCoNi, 11: Al0.5CrFeCoNi, 12: Ti2CrCuFeCoNi, 13: AlTiVYZr, 14: ZrTiVCuNiBe. [37]

size difference and large negative mixing enthalpies [40], which is the opposite of what is true for the formation of solid solution forming HEAs. These amorphous materials have interesting properties as well, but are out of the scope of this report.

Another rather successful criterion for whether there will be a simple phase in HEAs is given by Yang and Zhang [41]. This criterion comes from the competition between entropy and enthalpy as laid out in the previous section and is defined as $\Omega = \frac{T_m \Delta S_{\text{mix}}}{\Delta H_{\text{mix}}}$ where T_m is the weighted average melting temperature of the elements in the alloy. Larger values for Ω implies a greater probability of forming a simple disordered phase. The value $\Omega = 1.1$ is suggested as a threshold, over which simple disordered phases will form, if at the same time the atomic size difference is less than 6.6. These criteria are not without faults, and Tsai and Yeh [39] mentions that they have a new proposed parameter to be submitted that will solve this.

It is noted that these analyses are based on the as-cast state [39], meaning that for heat-treated HEAs, or HEAs made via for instance mechanical alloying (MA), these parameters might not be valid.

When discussing the subject of phase selection parameters it is worth mentioning the work done by Guo et al. to determine whether a phase will be of bcc type or fcc type [42]. They noticed that the stable phase was directly dependent on the valence electron concentration (VEC). For $VEC < 6.87$ bcc phase was stable while for $VEC \geq 8$ fcc phase was stable. In between there was a combination of both. This can be seen for some HEA systems in Figure 3.2.

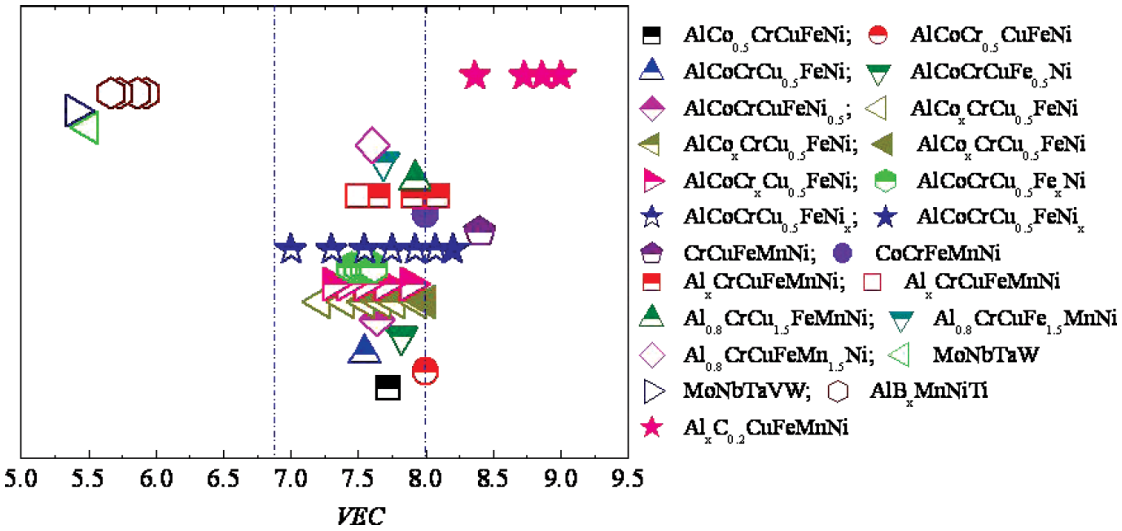

Figure 3.2: Relationship between VEC and the fcc, bcc phase stability for some HEA systems. Note on the legend: fully closed symbols for sole fcc phases; fully open symbols for sole bcc phase; top-half closed symbols for mixes fcc and bcc phases. [42]

3.2 Reasons for Properties

The special properties of HEAs (some of which will been described in section 3.3) are most often ascribed to four effects related to the high amount of the different alloy constituents. These are the *high mixing entropy effect*, the *sluggish diffusion effect*, the *lattice distortion effect* and the *cocktail effect*, which will all be described in the following sections.

3.2.1 High Mixing Entropy

The high mixing entropy effect has already been somewhat described in section 3.1.1. A higher amount of elements in a disordered state will give rise to an entropy that may suppress many intermetallic phases and other ordered phases, especially at elevated temperatures since the entropy contribution to the Gibbs energy in eq (3.1) scales with temperature while the enthalpy does not.

3.2.2 Sluggish Diffusion

It is easy to imagine that diffusion in HEAs works slower than conventional alloys. If one imagines a lattice built up of several different elements, then one atom diffusing from one spot to a neighbouring spot will most likely be in an environment quite unlike the one in the previous spot, with different elements in the neighbouring spots and therefore a different potential energy. It might very well be then that the potential energy in that spot is so much higher that the atom will return to its original spot. Of course it might as well be so that it is energetically preferable for the atom to ”continue” its journey

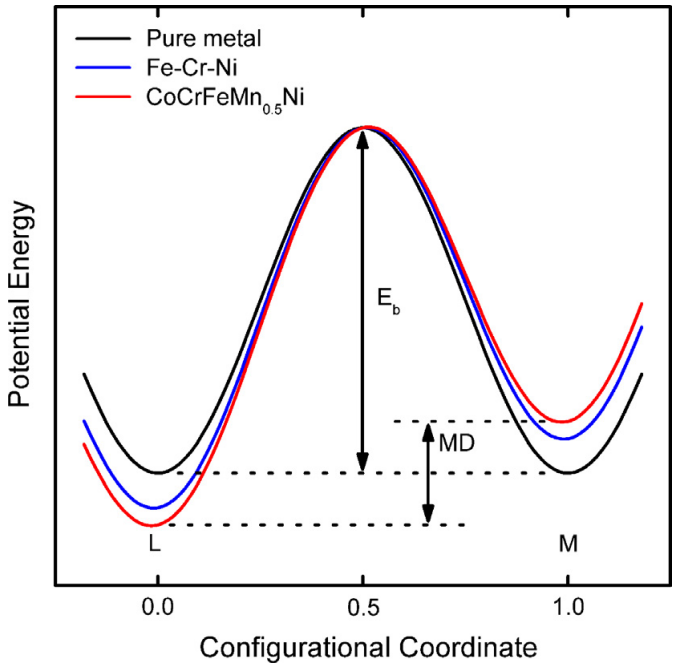

Figure 3.3: Schematic diagram of the variation of Lattice Potential Energy and Mean Difference during the migration of a Ni atom in different matrices. The MD for pure metals is zero, whereas that for HEA is the largest. [43]

another step, but there will also be spots where it will take more energy to pass i.e. the potential energy will fluctuate from spot to spot due to the different neighbouring elements.

Tsai et al. [43] showed this for CoCrFeMnNi, and in Figure 3.3 one sees the difference in potential energy between two neighbouring sites M and L for a nickel atom in a pure metal, a medium entropy alloy and a high entropy alloy. It is seen that for the pure metal the mean difference (MD) between the spots is zero while for the alloys there is a difference, which is higher for the high entropy alloy. Figure 3.4 shows the difference in diffusion coefficients for the different constituting elements in different matrices and Figure 3.5 shows the activation energies. Again it is easy to see that the diffusion is slower in HEAs.

Another fact leading to the sluggish diffusion is the fact that there is simply so many constituents. This means that there are a lot of different elements which will have to diffuse in a coordinated way, while facing the fluctuating potential energy mentioned above.

This sluggish diffusion indicate that many HEAs can have excellent high-temperature properties, with good creep resistance and strength properties (as will be discussed in section 3.3.2). It might however become troublesome when one wants a homogeneous alloy from casting, since the slow diffusion implies that it will stay segregated for a long time, even after long-time annealing.

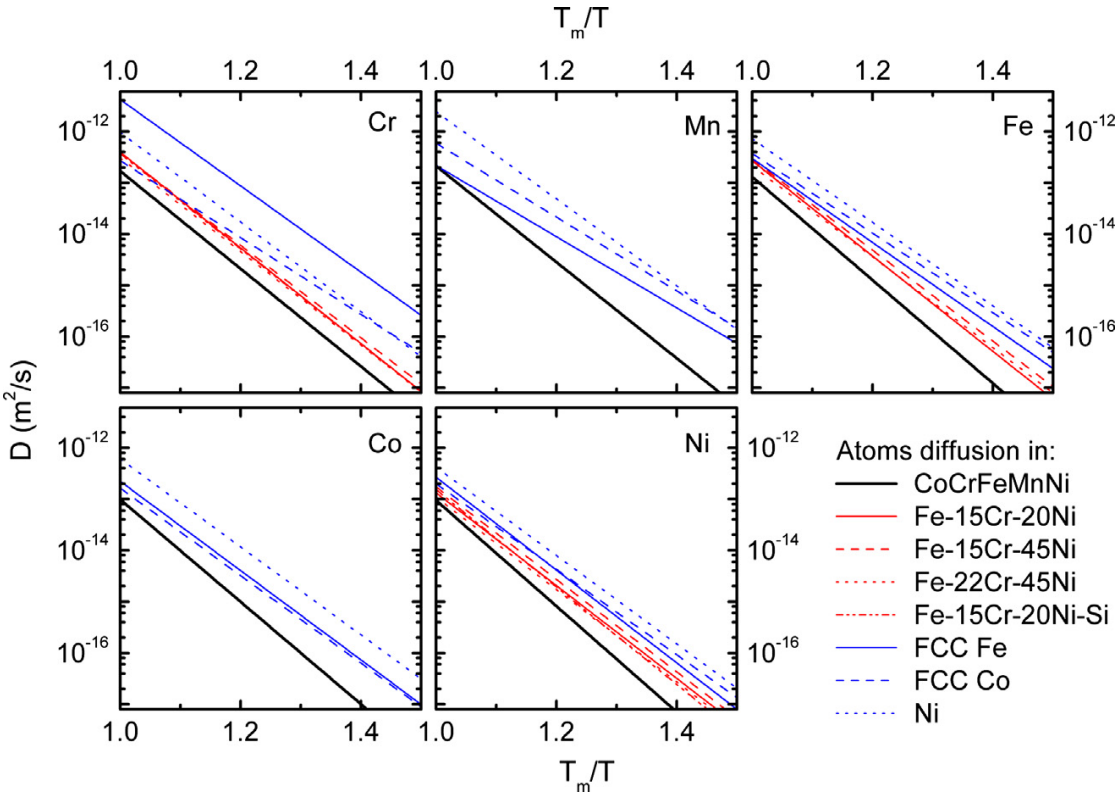

Figure 3.4: Temperature dependence of the diffusion coefficients for Cr, Mn, Fe, Co and Ni in different matrices. [43]

3.2.3 Lattice Distortion

A lattice consisting of atoms of different radii will become distorted, with larger atoms pushing on neighbouring sites and smaller atoms will have more free space in their vicinities. This distortion will hinder dislocation movement and thus lead to solid solution strengthening. As will be mentioned in later sections it will also increase the scattering of propagating electrons and phonons, meaning that the electrical and thermal conductivities will be lowered.

3.2.4 Cocktail Effect

The last of the four core effects is the cocktail effect. Basically it says that the properties of HEAs can not just be taken from averaging the properties of the constituting elements. There will also be some effects on the properties from the interaction between different elements and phases as well as from the lattice distortion effect, which at first may seem unintuitive. This cocktail effect then gives many possibilities for materials with different properties.

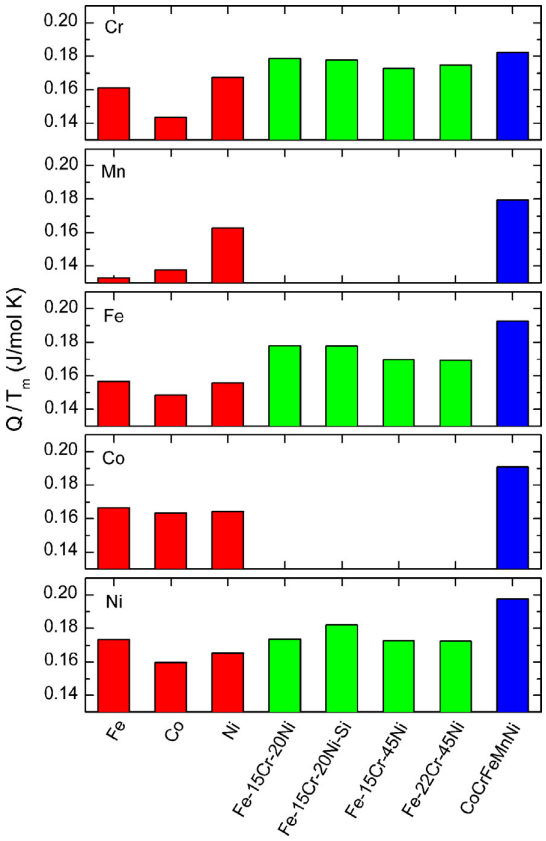

Figure 3.5: Normalized activation energies of diffusion for Cr, Mn, Fe, Co and Ni in different matrices. [43]

3.3 Typical Properties

In this section typical mechanical and physical properties of HEAs will be reviewed. It should be noted that most properties will be for some derivations of the Al-Co-Cr-Cu-Fe-Ni system, partly due to the simple reason that this is the most studied system, but also (as mentioned in section 2.4) since the constituents in the Al-Co-Cr-Cu-Fe-Ni system is largely the same as in the common superalloys, thus making this system a natural extension of superalloys.

To have something to compare the properties values with, Table 2.4 has some key values for nickel-based superalloys Inconel 718, Waspaloy and Haynes 230. Inconel 718 and Waspaloy are precipitation hardened superalloys (Waspaloy is a common replacement when the temperature is to high for Inconel 718), while Haynes 230 is a solution hardened superalloy, and will be a bit more relevant in comparing with most HEA properties since most of these are solution hardened as well.

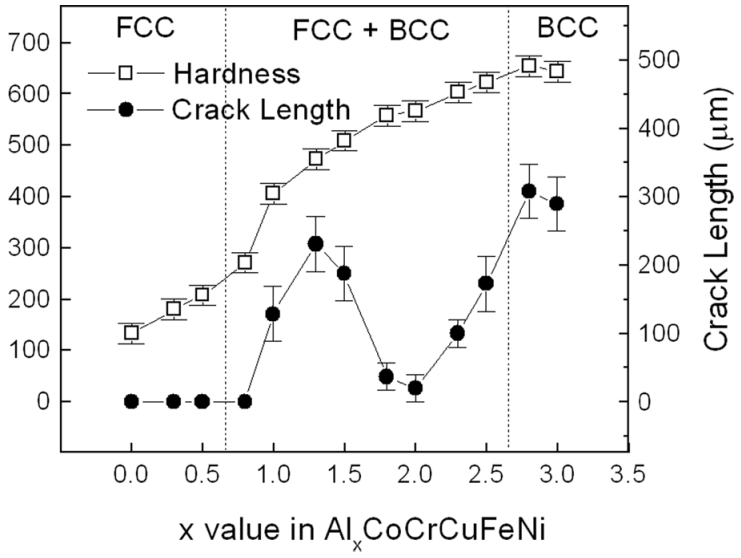

Figure 3.6: Vickers hardness and total crack lengths of the Al_xCoCrCuFeNi alloy system with different aluminum contents (x values in molar ratio). [44]

3.3.1 Room Temperature Strength

Al-Co-Cr-Cu-Fe-Ni

The strength of the AlCoCrCuFeNi-system is one of the more studied set of properties for HEAs [44, 45, 46, 47, 48]. Early studies showed the strength properties for varying content of aluminium for the arc-melted and cast system [44], and since changing the aluminium content will change the crystal structure of the alloy [42] this will change the strength. Ordinarily a fcc phase is softer and more resistant to change under elevated temperatures while a bcc phase is harder and more sensitive to high temperatures. For lower Al content there is a rather ductile fcc phase while increasing it will introduce an ordered bcc phase which will increase in volume with more Al and thus increase the strength of the alloy while lowering its ductility. The hardness ranges from $\approx 100 - 600$ HV with lower values for higher volumes of fcc phase and vice versa (see Figure 3.6). The strengthening is attributed to solid solution strengthening with the larger Al-atoms, precipitation strengthening of nanophases as well as increasing the ratio of the stronger bcc phase [44]. The alloy has a high strength at elevated temperatures up to 800 °C.

Heat-treatments such as multi-step-forging [45], annealing [46] and aging [47] at different temperatures can alter the properties. Forging increases tensile yield strength, ultimate tensile strength and ductility to 1040 MPa, 1170 MPa, 1 % from 790 MPa, 790 MPa, 0.2 % for the arc-melted and cast AlCoCrCuFeNi and lowers the brittle to ductile transition temperature from $700 - 800$ °C to $600 - 700$ °C. Aging above 645°C gradually changes the bcc structure to fcc, lowering the yield strength but increasing the plasticity. As for annealing it increases the fcc phase as well, making it a possible control-tool for the volume ratio between the fcc and bcc phases. Heat-treatments will also affect the

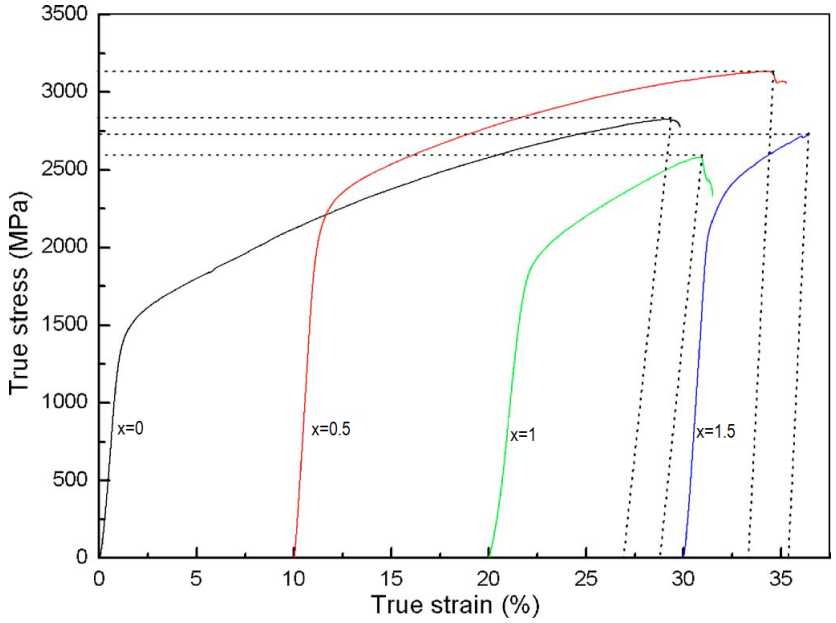

Figure 3.7: Compressive true stress-strain curves of AlCoCrFeNiTi$_x$ alloy rods with diameter of 5 mm. [54]

modulus of elasticity E [48], which in the as-cast state has been shown to be 180 GPa, which is lowered to 95 GPa after 0.5 hour of annealing at 550 °C. Extending the annealing to 2 hours again increases E to 115 GPa. The lowest E was achived for the splat-quenched alloy, 40 GPa.

Similar characteristics is seen for the copper-free version, AlCoCrFeNi, which also had its properties studied [49, 50, 51]. It is a bit stronger than AlCoCrCuFeNi since copper often segregates to the interdendrite regions [52, 53]. An interesting alloy worthy of mention here is the AlCoCrFeNi$_{2.1}$ *eutectic* HEA, designed to have a lamellar fcc(soft)/B2(hard) eutectic microstructure [51]. It shows good tensile properties, both at room temperature and elevated temperatures, with a true fracture stress and true strain of 1186 MPa and 22.8 % at RT and 538 MPa and 22.9 % at 700°C. Its strength is also shown to increase after cold rolling, with higher fracture stress but lower strain.

The effect of adding of titanium to either the AlCoCrCuFeNi or the AlCoCrFeNi system has been researched as well [52, 53, 54, 55, 56, 57]. For low amounts of Ti in the system without copper there are two bcc phases. For higher concentrations of titanium a Laves phase forms. It shows a high strength (Figure 3.7 shows the true stress strain curves for AlCoCrFeNiTi$_x$ for some values of x). Particulary, the AlCoCrFeNiTi$_{0.5}$ alloy has a compressive yield strength of 2.26 GPa, a fracture strength of 3.14 GPa and a plastic strain of 23.3 % [54]. This system gets its strength from among other factors bcc solid solution strengthening, precipitation strengthening and nano-composite effects [56, 57]. If the concentration of Co is raised one of the two bcc phases transforms to a fcc which lowers the strength but also the ductility [56].

Mn addition can in some scenarios contribute to great age hardening, such as with $Al_{0.3}CrFe_{1.5}MnNi_{0.5}$ and $Al_{0.5}CrFe_{1.5}MnNi_{0.5}$ where a hardness of 850 HV is reached [58] due to the bcc matrix transforming into a Cr-Mn-Fe σ phase (a phase with the same tetragonal structure as σ-CrFe) with the same composition [59]. This happens rather quickly since it is not particularly dependent on diffusion. The high softening resistance for $Al_{0.5}CrFe_{1.5}MnNi_{0.5}$ is also worth mentioning, being higher than that of high-speed steels [58]. The addition of Mn to the system without aluminium and copper has also been studied, and it was found that the tensile yield strength is slightly increased (from 140 MPa to 210 MPa [60, 61]), but with lowered ductility. The increase in strength is attributed to the lattice strain effect of having multiple principal elements. All in all the alloy is rather soft and ductile [60], but tensile strength can be increased by treatments based on lowering the grain size [62].

Mo has been added to both AlCrCoCuFeNi [63] and AlCrCoFeNi [64]. The effects were similar for both alloys. For low Mo contents the original phase structure is maintained, while for a bit higher Mo addition, a secondary phase (referred to as the α phase in Refs. [63] and [64]) was formed, which then grew in volume with increasing amounts of Mo. The alloy without copper exhibited the best mechanical properties, both for tensile and compressive tests. Yield strength ranged from 1051 to 2757 MPa and compressive fracture strength ranging from 2280 to 3036 MPa as $AlCrCoFeNiMo_x$ had x going from 0 to 0.5. The strengthening is attributed to solid solution strengthening by the Mo-atoms and precipitation strengthening of the α phase.

Nb added to AlCrCoFeNi leads to a Laves phase beside the bcc solid solution. This then, as can be expected, leads to an increase in yield strength and hardness along with a decrease in plasticity. Taking the Nb-content from 0 to 0.5 increases the yield strength from 1373 to 2473 MPa while decreasing the plastic strain limits from 24.5 to 4.1 %. The hardness is found to follow the Nb-content linearly according to $HV = 454x + 530$, where x is the niobium concentration [65].

For $AlCrCoFeNiSi_x$ where x ranges from 0 to 1 there is an increase in strength with increasing Si but a lowering in plastic strain. The best combination is seen for $x = 0.4$ which reaches a (compressive) yield strength of 1481 MPa, fracture strength of 2444 MPa and plastic strain 13.38 %. The phase of the alloy system is mainly a bcc solid solution, with increasing silicon concentration leading to a secondary phase (referred to as the δ phase in Ref. [66]) precipitating at the grain boundaries which in turn changes the fracture type from plastic to brittle. The increased strength is attributed to solid solution strengthening with the Si atoms along with precipitation strengthening of a nanoscale cellular structure [66].

Refractory HEAs

Refractory metals, with their high wear resistance and high melting point, has been used as components in several high-entropy systems. A lot of work has been done in Dayton, Ohio by Senkov et al. [67, 68, 69, 70, 71, 72, 73, 74, 75], but there has also been other groups studying these interesting systems [76, 77, 78].

Most of the refractory alloys studied by Senkov show high hardness and strength.

Compressive yield strengths range from 900 [72] to 2000 MPa [74], and the hardness ranges from 3 to 5.8 GPa respectively. All alloys show mainly a bcc solid solution [69, 76, 77, 78], but for some there is also intermetallics [78] and/or other bcc phases. The strongest alloy for instance, $AlMo_{0.5}NbTa_{0.5}TiZr$ has two bcc phases with similar lattice parameters but different composition. These phases form a nano lamellae modulated structure which (along with Al's strong bonding with other elements) is seen as the reason(s) for the unusually high strength and hardness for this particular alloy.

Even though these refractory HEAs are mostly rather brittle (being mostly bcc-type) [67, 71, 73] but there are some showing a rather high compression ductility (> 50%) [69, 73, 76]. Stress-strain curves for the aluminium containing refractory alloys at different temperatures can be seen in Figure 3.8.

Other systems

Zhou et al. studied the $Al_x(TiVCrMnFeCoNiCu)_{100-x}$ system [79]. It goes through similar phase changes as AlCoCrCuFeNi with the changing of the aluminium content, except at different values for x along with the fact that for higher x intermetallic phases precipitate. It shows generally good compressive properties, which is attributed to solid solution strengthening of the aluminium atoms along with replacing the more ductile fcc phase with a bcc phase. The best compressive strength, 2.431 GPa, occurs when $x = 11.1$.

There has also been some research going into finding low density HEAs [80, 81], with some promising results. AlNbTiV [80], with a density of 5.59 g/cm^3, which has a coarse grained single bcc phase. It has a good compressive yield strength at room temperature, 1020 MPa as well as at elevated temperatures (685 MPa at 800 °C), but poor room temperature ductility, which is blamed on the aluminium forming strong chemical bonds with the other elements. The aluminium bonding is however also attributed as the source for the good compressive yield properties. $Al_{20}Li_{20}Mg_{10}Sc_{20}Ti_{30}$ [81], produced via MA, with a density as low as 2.67 g/cm^3 also shows promise. After MA it has a single phase fcc structure with a hardness of 5.9 GPa, which after annealing is changed to a single phase hcp structure, now with a hardness of 4.9 GPa. By estimating strength as hardness divided by three, $Al_{20}Li_{20}Mg_{10}Sc_{20}Ti_{30}$ shows a specific yield strength comparable to that of SiC, though being a metal it should exhibit more ductility and other metallic properties. Its high hardness is partly attributed to its nanocrystalline grain sizes.

3.3.2 Elevated Temperature Strength

The elevated temperature properties of HEAs have been somewhat studied for different systems. $Al_xCoCrCuFeNi$ is shown to have rather good compressive properties (see Figure 3.9), specially for lower values of x where it has a more temperature resistant fcc structure [44]. Forging the alloy makes it softer and more deformable at elevated temperatures [47]. Tensile properties at elevated temperatures can be seen in Figure 3.10. The high temperature tensile properties for the eutectic $AlCoCrFeNi_{2.1}$ was already mentioned in section 3.3.1.

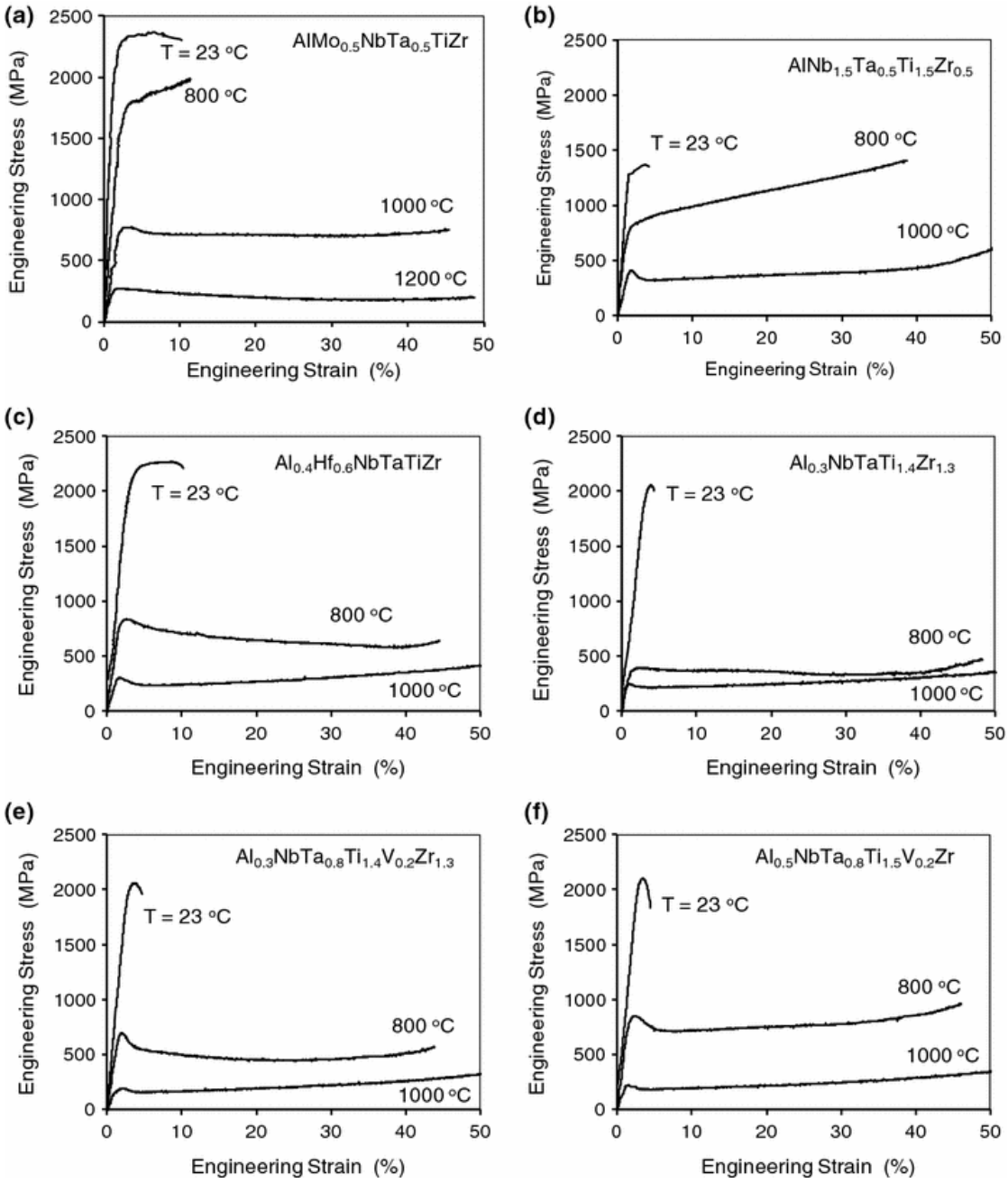

Figure 3.8: Engineering stress–strain deformation curves of six refractory HEAs containing aluminium. [75]

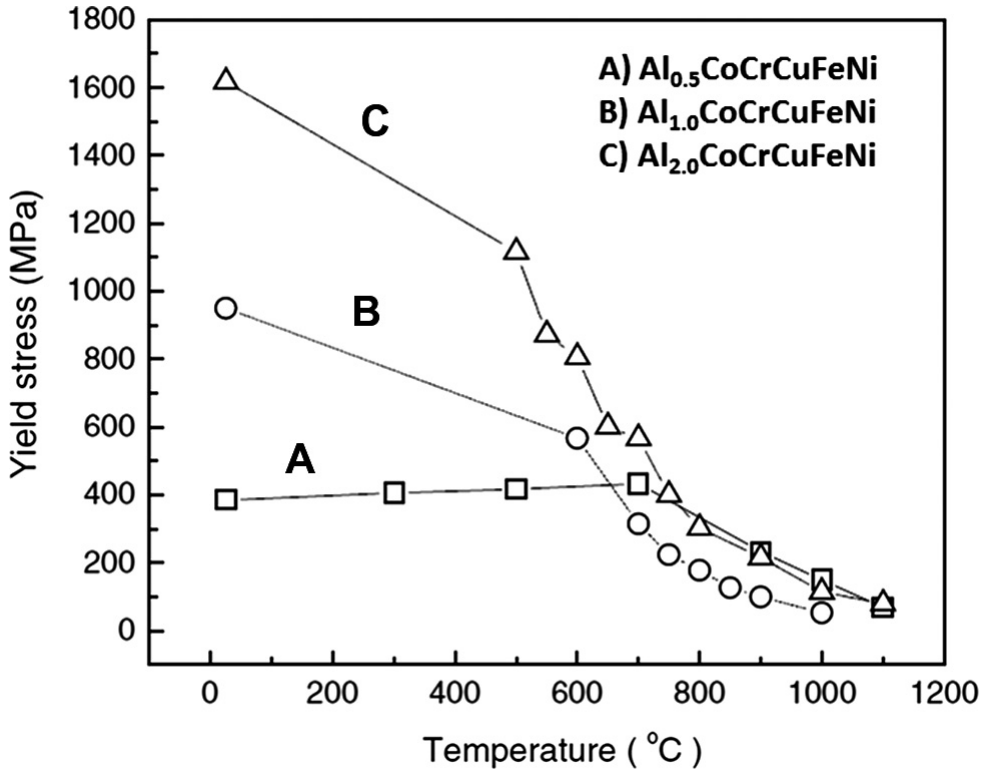

Figure 3.9: Compressive yield strength of $Al_xCoCrCuFeNi$ alloy system tested at different temperatures: (A) $Al_{0.5}CoCrCuFeNi$, (B) $Al_{1.0}CoCrCuFeNi$, and (C) $Al_{2.0}CoCrCuFeNi$ alloys. [32]

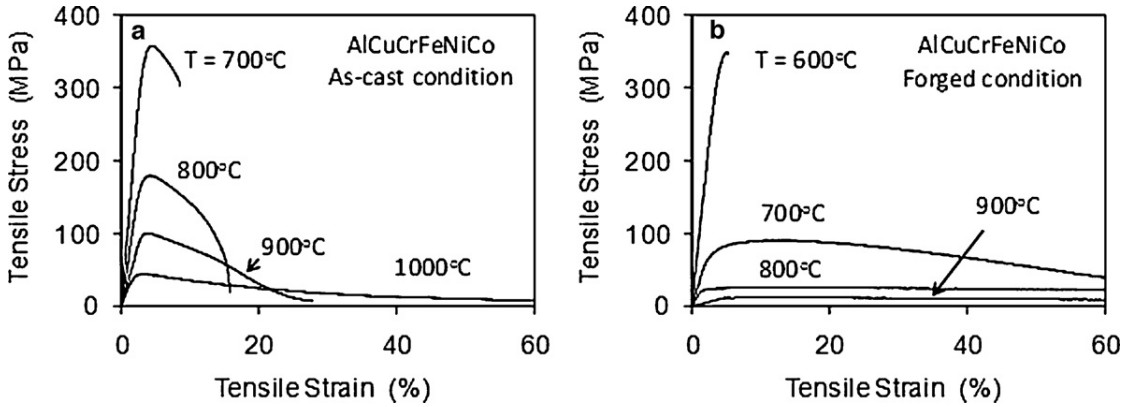

Figure 3.10: Typical stress–strain curves of the as-cast (a) and hot forged (b) AlCoCrCuFeNi samples deformed at different temperatures and the initial strain rate of $10^{-3}s^{-1}$. [47]

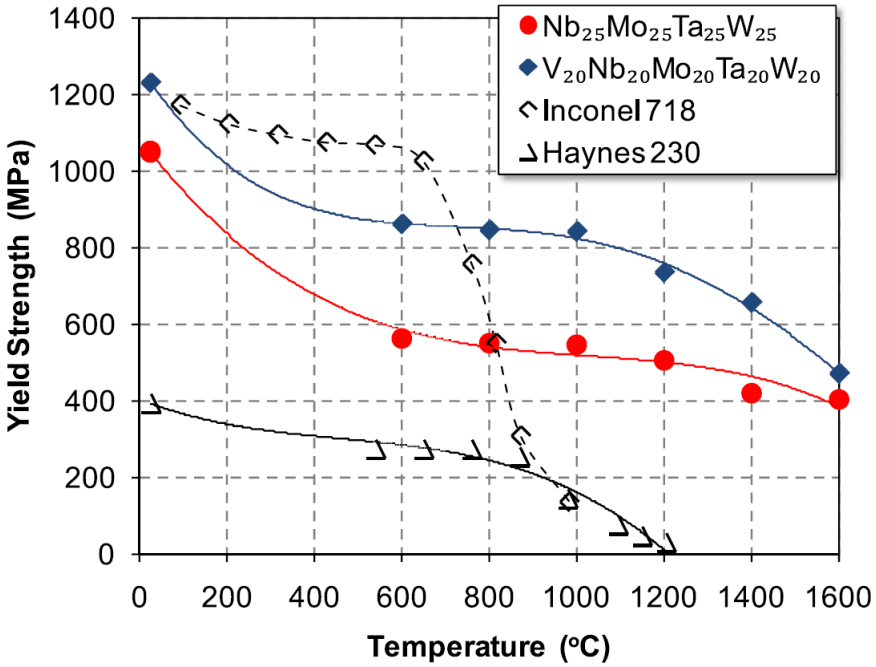

Figure 3.11: The temperature dependence of the yield stress of NbMoTaW and VNbMoTaW HEAs and two superalloys, Inconel 718 and Haynes 230. [67]

As for the refractory alloys most of them show high strength at elevated temperatures, especially the aluminium-containing refractory alloys produced by Senkov et al. [74, 75]. These alloys have comparatively low densities, and their specific yield strength can be seen along side those of AlCoCrCuFeNi and some conventional superalloys in Figure 3.20 and their engineering stress-strain curves can be seen in the above mentioned Figure 3.8. Figure 3.11 shows a yield strength comparison between two of the earliest refractory alloys, VNbMoTaW and NbMoTaW and two conventional superalloys Inconel 718 and Haynes 230. In the figure it is easily seen that while Inconel 718 has better strength properties at lower temperatures, HEAs maintain their properties to a higher degree for temperatures above 600 °C.

As mentioned earlier many HEAs show a lesser degree of softening than conventional alloys at elevated temperatures [58, 82, 83, 84, 85]. Generally deformation seems to happen in two different ways, depending on whether the temperature is above or below a certain (material dependent) transition temperature. Below this temperature the main deformation method is often slip, and above it is of a diffusional type [82, 83]. HEAs with their solid solution strengthening is rather resistant to slip deformation, even at higher temperatures. As for the deformation at temperatures above the transition temperature this is somewhat hindered by the sluggish diffusion effect in HEAs (see section 3.2.2). This, among other properties, makes HEAs suitable for high temperature usage.

The steady state flow properties at elevated temperatures ($1023 - 1123\,\mathrm{K}$) has been decided for FeCoCrNiMn [86], and two strain-rate dependent regions was found, where

for a rate below $2 \cdot 10^{-5}\,\mathrm{s}^{-1}$ there was a drag of gliding dislocations, and the process was controlled by the diffusion of one of the constituents acting as a solute. For strain rates above $2 \cdot 10^{-5}\,\mathrm{s}^{-1}$ there was dislocation climb, and this was controlled by the diffusion of Ni (which was shown in [43] to be the slowest diffuser in the system). The fact that at elevated temperatures the initial simple fcc-structure changed to one with Cr and Mn-enriched precipitates lowered the mechanical strength. This was particularly notable for the slower strain rate samples, where the alloy was exposed to the higher temperatures for longer times due to the slow strain rate.

3.3.3 Wear Resistance

There has been several investigations into the wear resistance of different HEAs [44, 87, 88, 89, 90, 91]. Most of the work has been done on versions of the Al-Co-Cr-Cu-Fe-Ni system and it has been found, among other things, that contrary to the ordinary case with for instance ferrous alloys where wear resistance often goes linearly with hardness, for this system it sometimes seems independent [44, 88, 91]. This leads to HEAs with comparatively low hardness having high wear resistance (and vice versa). For instance $Al_{0.5}CoCrCuFeNi$ with a hardness of HV 223 has a wear resistance similar to that of SKD61 steel, which has a hardness HV 567 [44], as can be seen in Figure 3.12. This high wear resistance is attributed to surface hardening of the ductile fcc phase during wear test.

The type of wear has been shown to be dependent on aluminium concentration [87] and titanium concentration [89], where for low Al and Ti concentrations it is delamination wear and for higher concentrations it is oxidation wear (this is also related to the phases, with delamination in fcc phases and oxidation in bcc). Some vanadium can also increase the wear resistance [88] while increasing the iron concentration lowers both hardness and wear resistance (though for high rates of iron they do not decrease linearly).

$Al_{0.2}Co_{1.5}CrFeNi_{1.5}Ti_{1.0}$ is an example of an HEA with extremely good wear resistance, twice the wear resistance of SKH51 and 3.6 times the resistance of SUJ2 while having a hardness similar to that of SUJ2 [89]. This alloy also shows superior hot hardness.

3.3.4 Fatigue Properties

With fatigue, the only real measurements so far are on $Al_{0.5}CoCrCuFeNi$ [92, 93] and $Al_{7.5}Cr_{22.5}Fe_{35}Mn_{20}Ni_{15}$ [93]. The results compare favourably to among others steel alloys and titanium alloys. $Al_{0.5}CoCrCuFeNi$, consisting of two fcc phases, has a fatigue endurance limit between 540 and 945 MPa and a ratio between the fatigue endurance limit and the UTS calculated to between 0.402 and 0.703, while $Al_{7.5}Cr_{22.5}Fe_{35}Mn_{20}Ni_{15}$, with dendrite bcc and interdendrite fcc along with a dispersion of solution B2 Ni-Al particles, has a fatigue endurance limit between 540 and 630 MPa but due to the lack of UTS data the ratio is not calculated. Some scatter in the fatigue life was observed, and this is attributed to microstructural defects, and it is believed that reducing these will lead to a fatigue behavior better than that of conventional alloys. The endurance limits

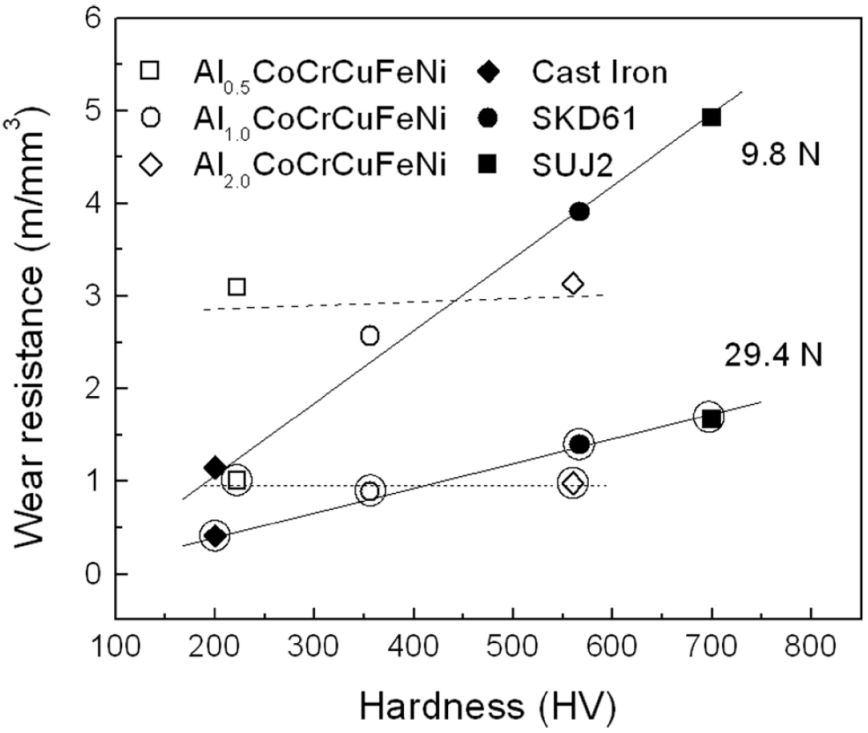

Figure 3.12: Wear resistance of the Al_xCoCrCuFeNi alloy system, cast iron, SKD61 steel, and SUJ2 steel (circled markers represent the tests under 29.4 N, those uncircled represent the tests under 9.8 N). [44]

and the fatigue ratios can be seen compared with conventional alloys and bulk metal glasses in Figure 3.13.

The fcc-type $Al_{0.5}$CoCrCuFeNi shows better fatigue resistance than the bcc-type $Al_{7.5}Cr_{22.5}Fe_{35}Mn_{20}Ni_{15}$, which still shows a good result compared to conventional alloys in Figure 3.13, showing the promise for the fatigue resistance of HEAs as compared to conventional alloys in general.

3.3.5 Corrosion

Corrosion properties of HEAs has been described in several works [94, 95, 96, 97, 98, 99, 100, 101, 102, 103, 104, 105, 106] and promising discoveries have been made. In general, HEAs show a range of corrosion properties, from good to not so good, in both H_2SO_4 and NaCl (see Figure 3.14).

The (mostly amorphous) AlCoCrCu$_{0.5}$FeNiSi HEA for instance shows a good corrosion resistance at room temperature, where it is more resistant than 304S stainless steel in both chloride and acid environments [94], though it should be said that this alloy is more susceptible to pitting corrosion in chloride environments than 304S. There is however no signs of pitting when in chloride free environments. When the temperature is

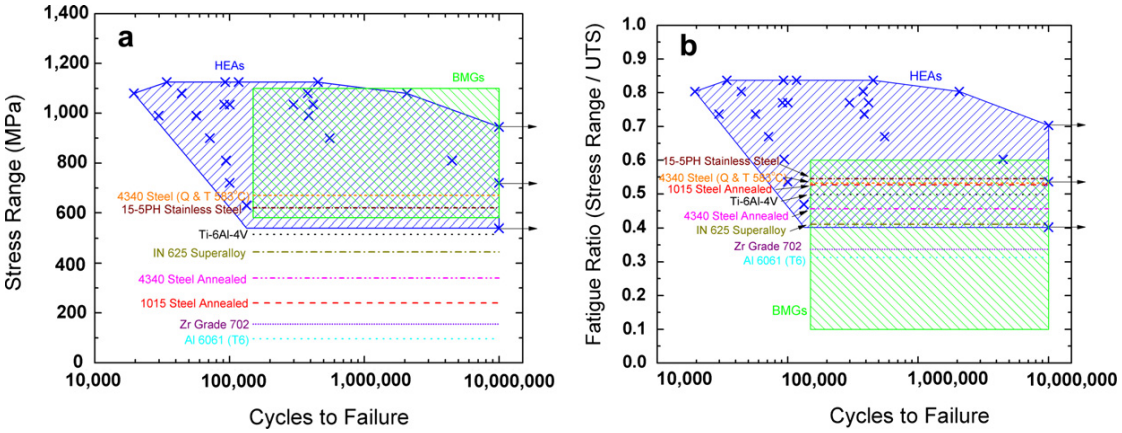

Figure 3.13: *S–N* curves comparing (a) the endurance limits and (b) the fatigue ratios of the $Al_{0.5}CoCrCuFeNi$ HEA, other conventional alloys, and BMGs. [92]

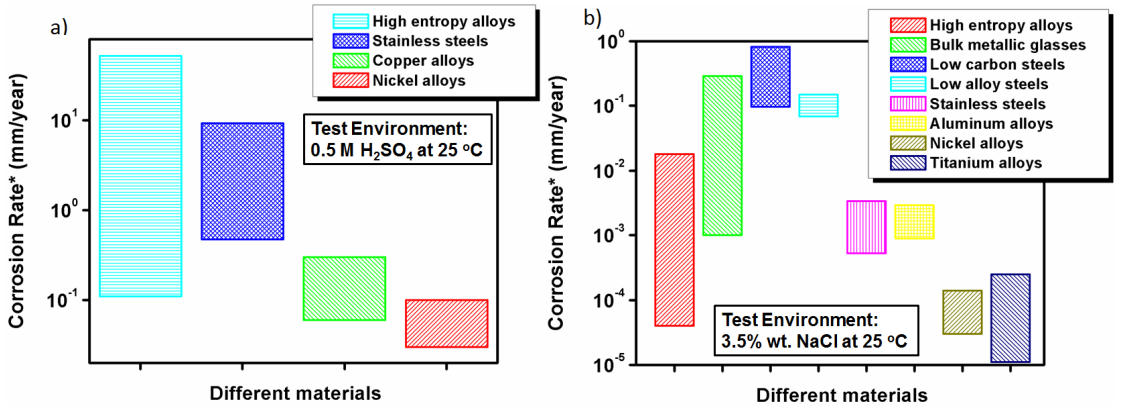

Figure 3.14: A comparison to average corrosion rates (mm/year) between HEAs and other materials in the (a) 0.5 M H_2SO_4 solution at room temperature (b) 3.5 wt.% NaCl solution at room temperature [106].

raised it shows a decrease in corrosion resistance [95], both for acid and chloride environments, though to a smaller extent in chloride in comparison with H_2SO_4 where it shows no tendency to passivate. The corrosion resistance in NaCl at elevated temperatures, with a lower activation energy and a smaller passive region than for 304S, indicates that for temperatures above room temperature 304S has better corrosion properties [95].

Studies on the corrosion behavior of copper containing HEAs shows that they often have worse corrosion resistance than alloys without copper, due to copper segregating into inter-dendrite regions giving rise to galvanic action between the dendrite and inter-dendrite regions [96, 99, 105]. This can however possibly be adjusted by aging the alloy at between 1100 and 1350° C and thus dissolving the copper into the dendrite [99].

Al also can show negative effects on the corrosion resistance, like for $CrFe_{1.5}MnNi_{0.5}$ [97], where the addition of Al lowers the corrosion resistance in acids and impairs the

pitting resistance in chloride environments. This does not say that the addition of Al always give poor corrosion resistance. $Al_{0.5}CoCrFeNi$ shows both lower corrosion potential and pitting potential than 304L stainless steel in NaCl [98], but here pitting resistance is impaired when aging between 350 and 950°C. The pitting resistance for this type of alloy can be increased by anodizing in H_2SO_4, at least when the Al content is 0 or 0.3, by creating a passive oxide film which protects against the pitting corrosion [102]. One reason for the lowering of the corrosion resistance in sulfuric acid by the addition of Al, at least above room temperature is the porous and inferior nature of the protection oxide film of Al in these alloys [103].

Adding boron in $Al_{0.5}CoCrCuFeNi$ lowers its corrosion resistance by producing Cr, Fe and Co borides, meaning that there is less Cr available. Mo in $Co_{1.5}CrFeNi1.5Ti_{0.5}$ lowers its general corrosion resistance in sulfuric acid [101] but increases the pitting resistance in NaCl [101, 104].

3.3.6 Oxidation

Some research have gone in to the oxidation properties of HEAs [58, 89, 90, 107, 108, 109, 110, 111, 112]. There are examples of HEAs which exhibit better oxidation resistance than ordinary alloys. For instance $Al_xCo_{1.5}CrFeNi_{1.5}Ti_y$ exhibits greater oxidation properties than both SUJ2 and SKH51 at both 600 and 800° C (the weight gain for which, when being exposed to the temperatures for 24 hours, can be seen in Figure 3.15) [89] and the refractory $NbCrMo_{0.5}Ta_{0.5}TiZr$ has better oxidation properties than commercial Nb-alloys [109].

Several thin films and coatings have been prepared and had their oxidation properties tested [107, 108, 110]. A laser cladding of Ti-6Al-4V by TiVCrAlSi is shown to improve its oxidation properties [107] and $(Al_{23.1}Cr_{30.8}Nb_{7.7}Si_{7.7}Ti_{30.7})N_{50}$ and $(Al_{29.1}Cr_{30.8}Nb_{11.2}Si_{7.7}Ti_{21.3})N_{50}$ has both been shown to have good resistance to oxidation [110]. The high temperature oxidation properties of (Ti-Zr-Hf-V-Nb)N coatings have been shown to improve if deposited under increased stress-strain [108].

In general Al [58, 110] and for refractory alloys Ti and Si [111] have been shown to improve oxidation properties, while Fe [90] (in general) and V [111] (at least for refractory alloys) have been shown to decrease them.

One might expect rather good oxidation resistance in general in the alloys containing both aluminium and chrome in rather high concentration, these being two elements that conventionally give good resistance in other alloys. Al does this by creating a protective aluminum oxide (Al_2O_3) layer on the surface and Cr does this by creating a protective chromium oxide (Cr_2O_3) layer on the surface.

3.3.7 Thermal Properties

There has not been much work done on thermal properties, such as the coefficient of thermal expansion (CTE) and the thermal conductivity $\kappa(T)$. The research done has been on the $Al_xCoCrFeNi$ system [113], and some results can be seen in Figure 3.16 for the thermal conductivity, where it can be seen that the thermal conductivity is similar

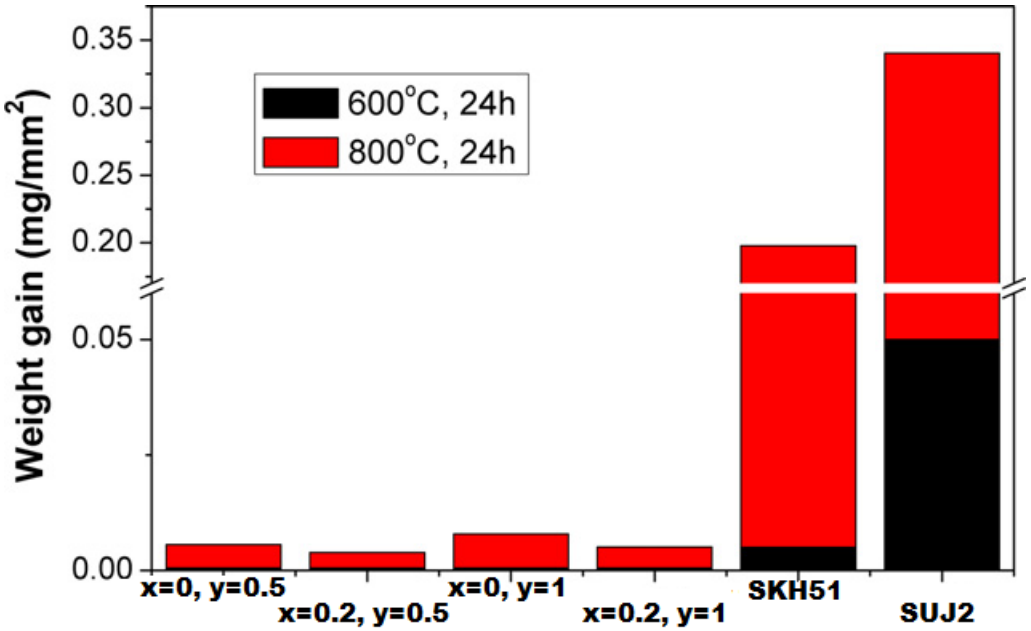

Figure 3.15: Weight gain test of $Al_xCo_{1.5}CrFeNi_{1.5}Ti_y$, SUJ2 and SKH51 specimens at 600 and 800°C for 24 h. The data is presented as weight increase per unit area after test. [89]

to that of the superalloys in Table 2.4, and Figure 3.17 for the CTE where one sees that at least for this alloy system there is a greater increase in CTE over temperature than in the superalloys given in Table 2.4. It is also found to depend on the Al concentration.

It has been found that as opposed to pure metals where thermal conductivity decreases with increased temperature it increases in HEAs. This is attributed to the increase in lattice size from thermal expansion, giving the electrons a larger mean free path before scattering, as well as due to a smaller carrier concentration, the carrier concentration decreasing with temperature and the lattice distortion effect, reducing the sensitivity of the thermal conductivity on the carrier concentration as compared to for pure metals [113, 114].

Overall the thermal conductivity for HEAs is lower than for pure metals, and this is attributed to the lattice distortion effect, which was described in section 3.2.3. A presence of nano-grains and precipitates, often arising from the casting of HEAs, will also reduce the thermal conductivity [85]. Figure 3.18 illustrates the different mechanisms responsible for lowering the thermal conductivity. Another difference for the thermal conductivity of HEAs to that of pure metals is that the electron contribution and phonon contribution to the thermal conductivity in HEAs is of equal magnitudes as opposed to dominated by the electron contribution [113].

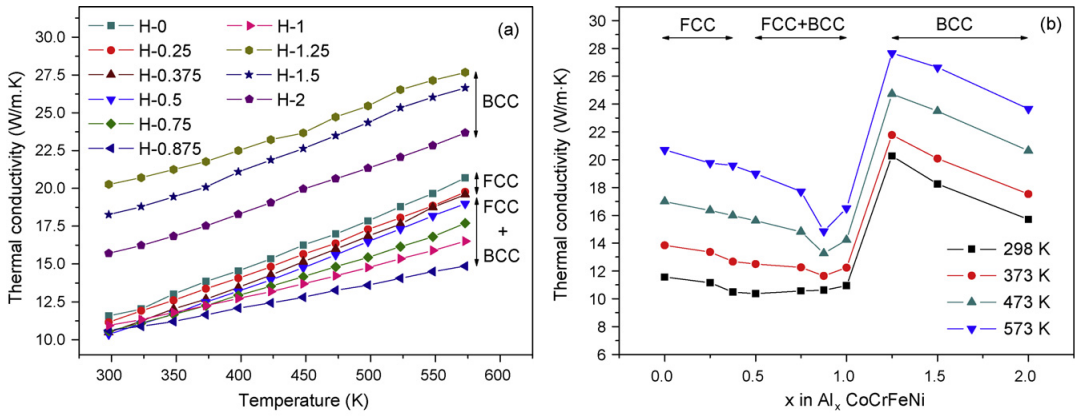

Figure 3.16: Diagrams for curves of thermal conductivity as a function of temperature (a), and as a function of x in $Al_xCoCrFeNi$ alloys (b), respectively. [113]

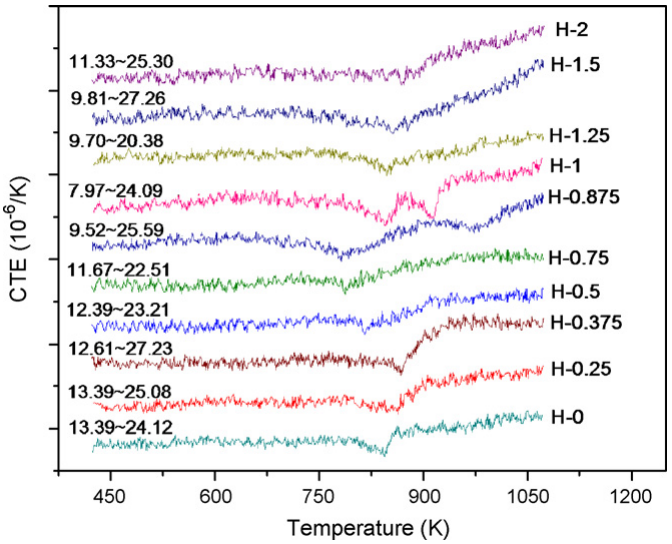

Figure 3.17: Variation of thermal expansion coefficient with temperature of $Al_xCoCrFeNi$ alloys. The maximum and minimum values are shown at the upper left-hand side of each curve, and the Curie temperature is shown in the gray region. Note that there is another "valley" for H-0.875 and H-1 in the figure. The interval in CTE coordinate is $15 \cdot 10^{-6}K^{-1}$. [113]

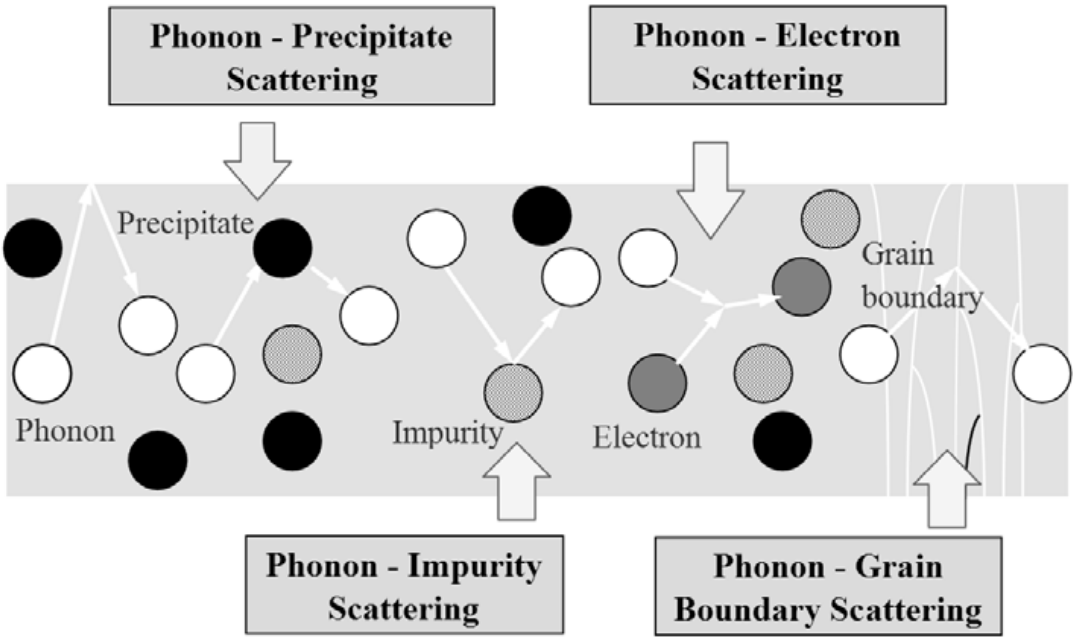

Figure 3.18: Schematic diagram depicting the mechanisms that reduce thermal conductivity in HE alloy coatings. [85]

3.3.8 Magnetic and Electric Properties

Magnetic properties of HEAs has been studied by several researchers [46, 115, 116, 117, 118, 119, 120, 121, 122, 123]. Most of these regards some versions of the AlCoCrCuFeNi systems [46, 115, 116, 117, 118, 119, 120, 121, 122] and it is seen that AlCoCrCuFeNi show good soft magnetic material properties with high saturated magnetization (M_s) and low coercivity (H_c) [46, 117, 119, 121], both of which increase after aging [116]. The ferromagnetic behavior of AlCoCrCuFeNi is seen to be correlated with the spinodal decomposition of the Cr-Fe-Co rich regions into ferromagnetic Fe-Co-rich and antiferromagnetic Cr-rich domains [116]. It is also seen that adding W makes it partially paramagnetic while adding Zr makes it completely paramagnetic [118]. A particular HEA seen as a possible contender as a new soft magnetic material is the $CoFeNi(AlSi)_{0.2}$, which shows a good combination of M_s, H_c and resistivity ρ [119, 122]. Generally the electrical resistivity is much higher than that of the relevant pure metals, and this is attributed to the lattice distortion effect [113, 115, 124], which was discussed more in section 3.2.3. It is also noted that after annealing the resistivity increases even more due to the appearance of more intermetallic phases [124].

As a curiosity it is worth mentioning that recently a superconducting HEA has been identified in $Ta_{34}Nb_{33}Hf_8Zr_{14}Ti_{11}$, with a critical temperature $T_c \approx 7.3\,\mathrm{K}$ [123].

3.4 Processing of HEAs

Of the different processing methods available for HEAs, the by far most common method is to melt and cast the alloy (as can be seen in Figure 3.19). The melting is most often done via vacuum arc melting, but sometimes via vacuum induction melting, followed by casting, often copper mold casting. [125]

It is worth noting the dependence of the microstructure on the processing conditions, such as the cooling-rate [126, 127, 128], heat treatments [46, 124], and forging [47]. An increased cooling rate has been shown to enhance the plasticity and strength in AlCoCrFeNi due to grain refinement and a reduction of Cr-segregation [126], the change in cooling-rate was achieved by casting alloys of different sizes, which also shows that the size will affect the properties somewhat. It should be said though that all samples had the same phase constitution. A comparison between "normal" cooling and splat quenching of AlCoCrCuFeNi has shown that the quicker cooling suppresses the growth of other phases and consists only of an imperfectly ordered bcc phase as opposed to several bcc phases and a fcc phase in the as-cast state [127]. This metastable phase is then sensitive to annealing, which would most likely bring forth the other phases which was suppressed during the quick cooling. Using the Bridgman solidification method for AlCoCrFeNi it has been noted that the dendrite changes to equiaxed grains, and this is attributed to the high ratio between temperature gradient and growth rate of this technique [128]. This dependence on processing conditions both increases the complexity of HEAs but also gives a greater ability to customize the properties. The fact that some HEAs have been shown to be forgeable is promising for the manufacturability of future alloys.

Another method to synthesize HEAs, where instead of going from a liquid to solid state starting with solid state constituents from the beginning, is to use mechanical alloying (MA), which is a PM method, followed by consolidation (most often spark plasma sintering). HEAs prepared by PM often show a greater homogeneity in their microstructure as compared to the segregated microstructure of melted and cast HEAs, which often exhibit dendrite and inter-dendrite regions, regions which can be hard to remove with homogenization due to the sluggish diffusion of HEAs. MA might also be preferable when dealing with elements with a wide range of evaporation temperatures, where some elements might be evaporated before others have melted. This might be averted during arc melting by placing the elements evaporating early below the other elements, but this is far from a foolproof method, and MA might be the better choice. It should be said however that it has been shown that the concentration of lighter elements is lower after MA than what was loaded in the apparatus, which is attributed to the lighter elements adhering to the walls during milling, and there has also been problems with achieving "full" homogeneity [129]. PM in general is a promising processing route, with both an increased probability of homogeneity and also the possibility nowadays to process rather large parts.

Coatings and thin films of HEAs has been prepared in several different ways. From a vapor state they have most often been prepared via either magnetron sputtering or plasma nitriding while from a liquid state they have most often been prepared via either

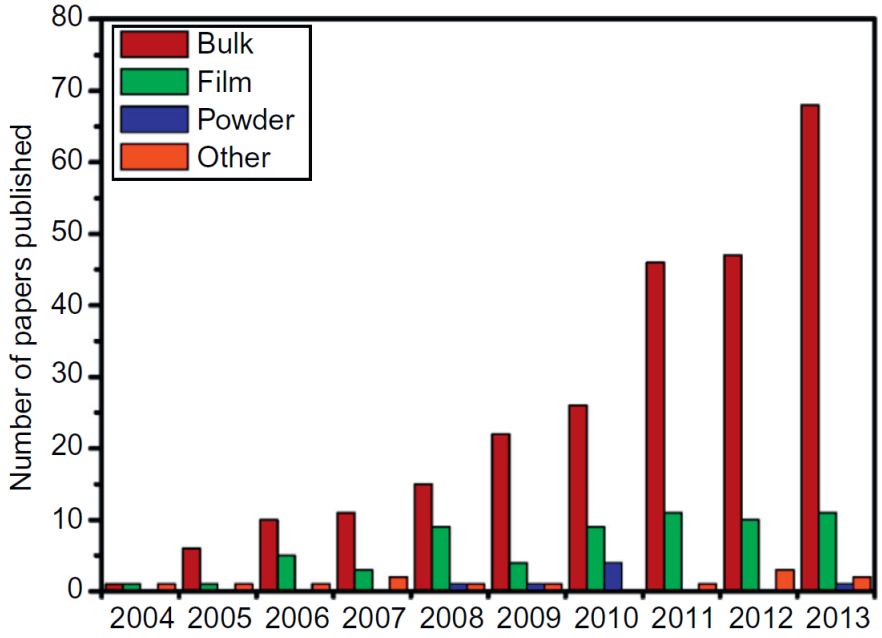

Figure 3.19: The number of papers published on HEAs that were produced by different processing routes. [125]

tungsten inert gas/gas tungsten arc welding (TIG/GTAW) or laser cladding (in both scenarios mostly on steel substrates).

There has also been some minor research into additive manufacturing of HEAs, where Y. Brif et al. [130] used selective laser melting (SLM) to synthesize FeCoCrNi. It was shown to contain only a single fcc phase, when synthesized over a range of processing parameters. The tensile properties was improved from the as-cast state, which is attributed to the fine microstructure achieved when using SLM. The tensile yield strength was 600 MPa when using a layer thickness of 20 μm, as compared to the 181 MPa obtained in the as-cast state. It was also rather ductile as could be expected from the fcc phase.

3.5 Motivations for Using HEAs as Aero Engine Materials

As seen in section 3.3 HEAs can compare favourably to many commercial alloys, especially at elevated temperatures. This is by itself good, but another major factor for the potential use of HEAs in aero engine materials is the possibility to lower the total density of the alloy with the capability to add greater amounts of lighter elements. Nickel-based super-alloys for instance are highly dependent on the density of Ni (8.908 g/cm^3 [3]). The most popular nickel-based alloy, Inconel 718 has a density of 8.19 g/cm^3 [29] while for instance the aluminium containing refractory alloy $AlMo_{0.5}NbTa_{0.5}TiZr$ has

Table 3.1: Densities for some HEAs and conventional alloys. † denotes that the density was calculated using the rule of mixtures in eq (3.3). It should be noted that the values used for ρ_i in eq (3.3) is based on the room temperature crystal structure of the pure element, which may not be the same as the crystal structure of the alloy. ‡ denotes a rule of mixtures density value calculation made by the researchers who measured the experimental value.

Alloy	$\rho\,(\mathrm{g/cm^3})$	**Alloy**	$\rho\,(\mathrm{g/cm^3})$
AlCoCrCuFeNi	7.1†	$AlMo_{0.5}NbTa_{0.5}TiZr$	7.4 [75]/7.3‡
AlCoCrFeNi	6.7†	$AlNb_{1.5}Ta_{0.5}Ti_{1.5}Zr_{0.5}$	6.88 [75]/6.8‡
$Al_{0.5}CoCrFeNi$	7.6†	$Al_{0.4}Hf_{0.6}NbTaTiZr$	9.05 [75]/9.0‡
CoCrCuFeNi	8.4†	$Al_{0.3}NbTaTi_{1.4}Zr_{1.3}$	8.18 [75]/8.1‡
$AlCoCrFeNiTi_{0.5}$	6.5†	$Al_{0.3}NbTa_{0.8}Ti_{1.4}V_{0.2}Zr_{1.3}$	7.78 [75]/7.7‡
$AlCoCrCuFeNiTi_{0.5}$	6.8†	$Al_{0.5}NbTa_{0.8}Ti_{1.5}V_{0.2}Zr$	7.42 [75]/7.3‡
$AlCoCrFeNiMo_{0.5}$	7.1†	NbMoTaW	13.75 [68]/13.6†
$Al_{0.3}CrFe_{1.5}MnNi_{0.5}$	7.2†	VNbMoTaW	12.36 [68]/12.3†
$Al_{0.5}CrFe_{1.5}MnNi_{0.5}$	6.9†	TaNbHfZrTi	9.94 [69]/9.89‡
$AlCoCrFeNiNb_{0.5}$	7.0†	$NbCrMo_{0.5}Ta_{0.5}TiZr$	8.02 [71]/8.23‡
$AlCoCrFeNiSi_{0.4}$	6.2†	NbTiVZr	6.52 [73]/6.50‡
$AlCoCrFeNi_{2.1}$	7.38 [51]/7.1†	$NbTiV_2Zr$	6.34 [73]/6.30‡
AlNbTiV	5.59 [80]/5.5†	$Al_{20}Li_{20}Mg_{10}Sc_{20}Ti_{30}$	2.67 [81]/2.7†
Ti-6Al-4V	4.43 [131]	CrNbTiZr	6.67 [73]6.70‡
Inconel 718	8.19 [29]	CrNbTiVZr	6.57 [73]6.52‡
Waspaloy	8.20 [27]	Haynes 230	8.97 [28]

a density of $7.4\,\mathrm{g/cm^3}$. The possibility to lower the density with increased amounts of aluminium, Al having a density of only $2.7\,\mathrm{g/cm^3}$[3], is very enticing.

Using the rule of mixtures, the density for a *single-phase disordered solid solution* can be calculated according to

$$\rho_{\mathrm{mix}} = \frac{\sum_i X_i A_i}{\sum_i \frac{X_i A_i}{\rho_i}}, \tag{3.3}$$

where A_i is the atomic weight of element i and ρ_i is the density. The density of equi-atomic AlCoCrCuFeNi can then be calculated (using values for A_i and ρ_i from Physics Handbook [3]) to $7.1\,\mathrm{g/cm^3}$. Theoretical and experimental density values for other HEAs can be seen in Table 3.1. It should be noted that the values used for ρ_i is based on the room temperature crystal structure of the pure element, which may not be the same as the crystal structure of the alloy. The density can then be used to calculate the specific yield strength (SYS), which is the yield strength σ_y divided by the density for the material. The SYS for some HEAs over a range of temperatures can be seen in

Figure 3.20 compared with the values for some conventional superalloys. It is clear that if looking at just these values there is a great deal of promise in HEAs for the weight reduction.

Such a weight reduction is something highly sought-after in the aerospace industry since a lower density means a lower engine weight, which in turn reduces the demands on the wing carrying the engine which may lead to a greater total weight reduction meaning a lesser amount of fuel needed in total.

Another possible improvement from an environmental perspective is the fact that increasing the working temperature of the engine reduces the emissions. Thus finding alloys capable of keeping their properties at increased temperatures is a good way to be able to reach future climate goals. The sluggish diffusion effect for HEAs discussed in section 3.2.2 indicates that HEAs could be good candidates for use at these elevated temperatures.

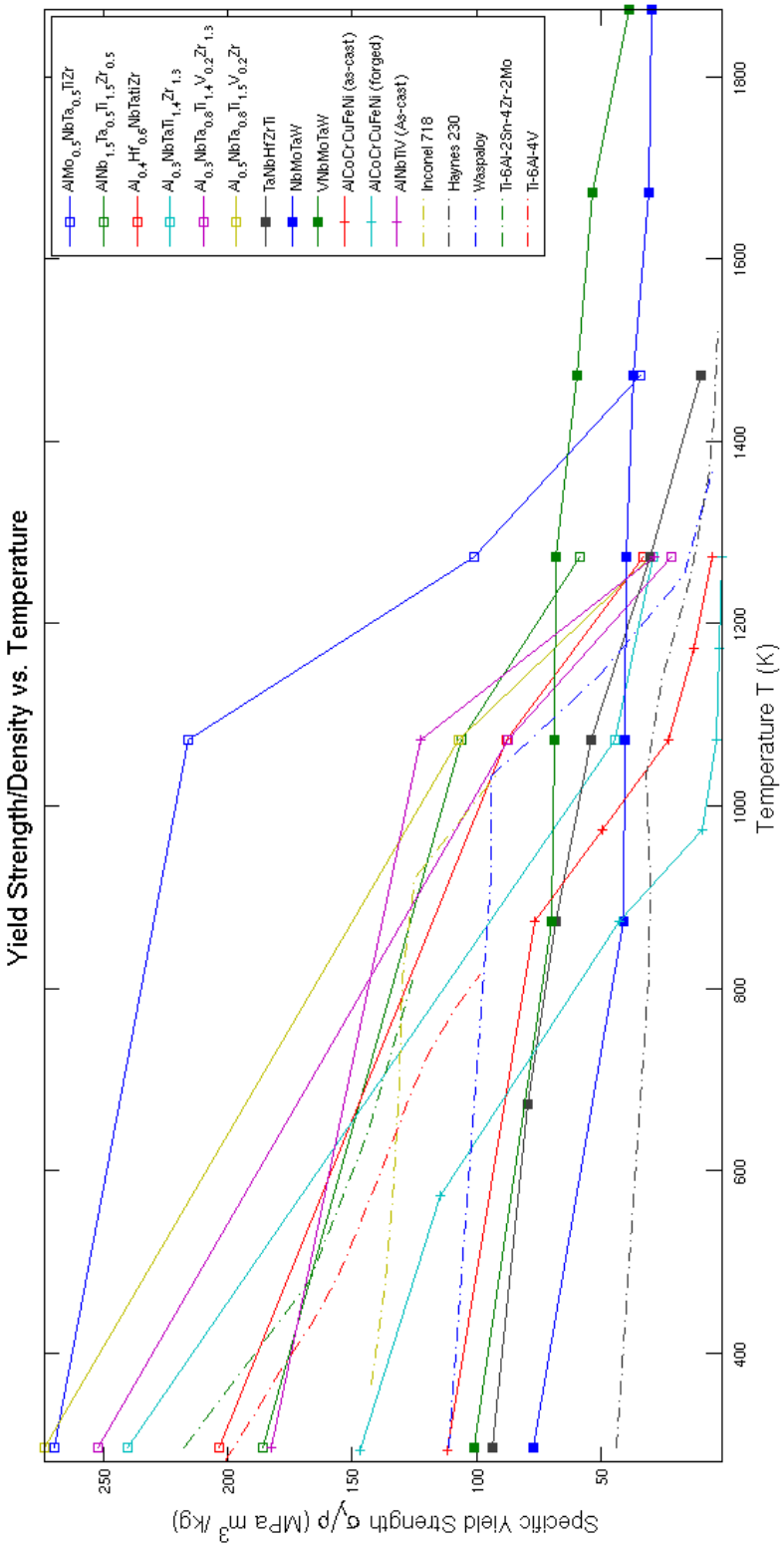

Figure 3.20: The specific yield strength for some refractory alloys (compressive strength, solid lines with square markers) [67, 69, 75], for AlCoCrCuFeNi (tensile strength, solid lines with cross markers) [47] AlNbTiV (compressive strength, also solid line with cross marker) [80], and for some conventional superalloys and titanium alloys (tensile strength, dashed lines) [27, 28, 30, 132, 133]. The density used for calculation of the specific yield strength for AlCoCrCuFeNi is the calculated one from table 3.1.

4

Bridging the Gap

With the many promising properties outlined in Chapter 3, especially at elevated temperatures, HEAs is an interesting new type of material. Being rather new, there are however still problems that remain to be solved before these types of materials can be used in aero engines. So far there has been a rather scattered research, with different properties examined for different systems made via different processing conditions. This is understandable with the amount of possible alloys that the high entropy concept gives. Using between 5 and 13 elements in equiatomic ratio gives 7099 possible alloys [32], and then varying the concentrations inside these systems gives rather many more possible combinations. It is really only the Al-Co-Cr-Cu-Fe-Ni system that has been studied under different conditions, and there is still a lot left to find out.

This chapter will give a summary of some of the more important properties left to study/problems left to solve, and this is from the perspective of what was learned in Chapter 2 regarding the demands of aero engines. Since it as mentioned is possible to have many different alloy systems, and the properties outlined in Chapter 3 is only for some of these, these ”remaining” properties are based on the systems that has already been studied. While one may expect some similarities in properties between the HEAs stemming from the high mixing entropy, lattice distortion and sluggish diffusion core effects, the cocktail effect still gives some uncertainty. Also considering the range in properties exhibited by conventional alloys, these more complex alloys are also expected to have rather varying properties.

The properties/problems that will be mentioned in this chapter is among others the strength versus ductility optimization, the lack of creep and fatigue tests, the problem with the coefficient of thermal expansion and the lack of information regarding machining.

4.1 Creep and Fatigue

As noted in section 2.4 two of the most important materials properties, are creep resistance and fatigue resistance. The research into these properties is at the moment rather lacking, with only one article and a master thesis (both by the same author) regarding the fatigue properties, which is on the fatigue properties of the $Al_{0.5}CoCrCuFeNi$ alloy [92, 93] and the $Al_{7.5}Cr_{22.5}Fe_{35}Mn_{20}Ni_{15}$ alloy [93], and while the results were promising for future materials at the moment the presence of defects in the materials tested gave a scattering of results. It should also be noted that the focus of the study was on HCF, while the most relevant property for the sought after parts in Chapter 2 is LCF. One thing noted between these two alloy systems is that the best fatigue resistance was shown by the fcc-based alloy, $Al_{0.5}CoCrCuFeNi$, rather than the alloy consisting of mainly a bcc but also some fcc phases. While these results is not enough to indicate a general trend, fcc-based HEAs are a good starting point when looking for fatigue resistant alloys.

The creep properties of HEAs also would benefit from more research. Even though, one might expect rather good properties due to the common strengthening mechanism of solution hardening as well as the sluggish diffusion in HEAs, which is quite resistant to the diffusional deformation at elevated temperatures as mentioned in section 3.3.2. While they might be promising, they still are not mapped yet, and this will be necessary before applying these alloys to turbine engines. If the creep properties is not good enough for the wanted alloy, conventionally a good way to increase the creep resistance is to coarsen the grain size, for instance by experimenting with the cooling rate of the alloy upon casting, or even perhaps experimenting with growing single crystal HEAs. This might be problematic however since many HEAs get their good strength (for instance [62, 74, 81, 126]) from their nanoscale grains, and coarsening these might negatively affect the strength.

4.2 Oxidation

Oxidation resistance is of importance for the aero engine and its specific parts, but often the relevant alloys have good oxidation properties from the beginning meaning this is seldom a limiting factor. For HEAs however, with the oxidation resistance still a rather unknown area, more research may be needed.

As mentioned in section 3.3.6 the alloys containing either aluminium, chromium or both in rather large concentrations is expected to have good oxidation resistance due to the creation of a protective layer, meaning that alloys based on the Al-Co-Cr-Fe-Ni system could be expected to have a good oxidation resistance. Refractory HEAs are of more interest for further studies, since refractory elements are known for their bad oxidation resistance. The refractory alloys with best mechanical properties also contain aluminium, and might thus create the protective Al_2O_3 layer, but more research is still needed (as it also is with the simpler Al-Co-Cr-Fe-Ni system). To summarize, for HEAs that need to exhibit oxidation resistance, aluminium and/or chromium are good candidates for constituting elements, but more research are needed to really understand

the oxidation properties of HEAs.

4.3 Thermal Properties

The good strength of HEAs at elevated temperatures is already noted. A potential problem with high temperature use however is the increase in CTE at higher temperatures, which is higher than that for conventional superalloys. This can be seen by comparing the data in section 3.3.7 and Figure 3.17 with that in Table 2.4 (but also note that the values in Table 2.4 are for 650°C = 923K, meaning that while there is a difference, it is not quite as big as it seems if one looks only at the max and min CTE in the figure). This may lead to problems if parts made out of these alloys are joined together with parts made by conventional superalloys in Table 2.4 if they expand and contract different amounts during a change in temperature. It should be noted that the CTE for HEAs has only been measured for the $Al_xCoCrFeNi$ system, and it might behave differently for other systems. The behavior of the CTE is especially important for HEAs that are considered for use as coatings, where it must match/complement the substrate material. It might not necessarily become a problem, but the stresses arising from thermal expansion/contraction will need to be in the minds of researchers.

Another potential problem that needs to be investigated is the thermal stability of HEAs. As described earlier many cast HEAs exist in metastable states, especially the HEAs prepared by fast cooling routes. Since the materials will serve at elevated temperatures for extended periods of time there is a risk that a phase change to the equilibrium state will occur. While the sluggish diffusion effect should hinder this from happening to some degree, the behaviour of HEAs at elevated temperatures for extended periods of time still needs to be further investigated since the thermal stability of the alloy is a necessity.

4.4 Property and Alloy Optimization

The need for optimization of properties for HEAs by modifying the composition and microstructure is most easily described in the competition between strength and ductility. As mentioned in section 3.3.1, when modifying the composition for an alloy system it is possible to increase/decrease the strength at the expense/gain of ductility when the phases changed according to composition. For certain compositions there might be a relatively weak but ductile fcc phase but modifying this composition may add a stronger but more brittle bcc phase or even a more brittle ordered phase. There will thus be a sort of competition between strength and ductility where one will have to optimize the properties for the relevant usage. This is not just a matter of strength and ductility since the other properties also depend on the microstructure and phase constitution, but the need for optimization is most easily illustrated by balancing strength against ductility. Also, most known strength have been measured under a compressive load, and only some under the more for engineering meaningful tensile load. The optimization of properties will have to be done by extensive research, but it should be possible to

make it less extensive by deciding on the crystal structure, phase constitution (whether one wants precipitation strengthening and such) and using the previously established empirical rules described in section 3.1.2.

It is also important to be aware of what elements that are to be used, rather than simply considering their effect on improving properties. Using rare or simply just very expensive elements will mean that the new alloy will become too expensive. This is important for instance with the low-density HEA $Al_{20}Li_{20}Mg_{10}Sc_{20}Ti_{30}$ [81], which, as can be seen, contains a large ratio of scandium, which is a rare and expensive element, and the alloy will be of little industrial interest.

4.5 Manufacturability

Another important property for a material is the ability to shape and join to other materials. If creating larger parts than the experimental samples will change the properties, it is also something that needs to be resolved, and Ref. [126] gives an indication that this is the case. Since HEAs are still a rather new type of material it is understandable that the process of manufacturing and shaping for industrial use has not been a number one priority, with other research taking precedence (for instance, understanding what composition and processing conditions will lead to which phase/phases).

As mentioned in section 3.4, HEAs have been made in several ways, mostly via casting but also some via powder metallurgy and different coating technologies. Forging of some HEAs has also been done, which is promising for further processing, but factors such as weldability is still unknown. So far a certain scattering in material properties has been noted (as mentioned in sections 3.3.4 and 4.1 regarding the fatigue studies). This scattering was attributed to defects in the material, and these types of defects need to be removed, or at least the amount of defects needs to be minimized.

Another example of property scatter is seen by looking at section 3.3.1, and particularly the articles where the compressive yield strengths for AlCoCrFeNi has been measured when adding Mo[64], Nb[65], Si[66] and Ti[54]. In all four cases the room temperature yield strength has been measured without the additional alloying element, and if one compares those yield strengths one sees that they are [64]:1051 MPa, [65]:1373 MPa, [66]:1110 MPa and [54]:1500 MPa, respectiveley. These, to be clear, are all for AlCoCrFeNi, without any additional elements. All four had their constituting elements arc melted on a water-cooled copper hearth followed by repeated remelting, and all four had a single bcc phase. A tighter control of the processing properties is thus needed to get reproducible results. This is even more important for those HEAs that have more than one phase, since the microstructure can be rather varied.

5

Summary and Future Prospects

High-entropy alloys are a new and promising type of alloys, with many exciting properties. While encouraging results have been shown, there are still as, mentioned in Chapter 4, many issues left to solve. This chapter will give a short summary of HEAs, which will be followed by a look into the future to see if they in fact are a potential material for aero engines, and especially the parts made by GKN Aerospace Engine Systems in Trollhättan.

5.1 Summary

HEAs is a new materials concept based on metallic alloys containing five or more principal components. This leads to many properties often attributed to the so called *four core effects*, the high mixing entropy, lattice distortion, sluggish diffusion and cocktail effects. That they consists of rather large concentrations of many different elements means that by including some lighter elements it is possible to create alloys with densities lower than those of, for instance, iron and nickel based alloys.

HEAs have a higher propensity to form simple solid solutions than was intuitively believed, and this is due to the high mixing entropy and sluggish diffusion effect. Several empirical rules to find whether a HEA will form a single solid solution or not has been suggested based mainly on the Hume-Rothery rules, and while they are rather useful there are still some problems. An empirical rule for finding if the phase will be either fcc or bcc based on the valence electron concentration has also been suggested.

Most of the research into HEAs has been done on some variations of the Al-Co-Cr-Cu-Fe-Ni system, and thus most of the summarized properties are given for this system. Some properties are however expected to be more general, especially those based on the lattice distortion and sluggish diffusion.

Many HEAs show a high strength, attributed partially to the lattice distortion, and the high strength can be somewhat retained at elevated temperatures, in part due to

the solid solution strengthening and in part due to the slow diffusion mechanism. The strength can be customized by changing the alloy composition which in turn will change the phase(s) of the alloy. It has been shown that for instance the CrCoFeNi system can be changed from fcc to bcc by adding Al. Other alloying elements can introduce even more complex phases which can strengthen the alloy, often at the expense of ductility. Alloying elements however will not always create new phases, since they can also diffuse into the existing phases and give solid solution strengthening.

HEAs have also shown good wear properties, with good softening resistance. As opposed to the conventional scenario where hardness and wear resistance have a linear dependence, for HEAs there is not always such a dependence. The type of wear has been shown to be dependant on the concentration of various alloying elements, changing between delamination and oxidation. There has not been much research into the fatigue properties of HEAs, the few results there seeming to be promising but there is a lot left to do.

The corrosion resistance varies with alloy composition, but overall it does not seem to be as good as that of nickel-based alloys. Some oxidation studies has been done, and they gave promising results. Another promising factor is that many HEAs contain rather large amounts of aluminium and chromium, which should increase the oxidation resistance. Chromium should also be good for the corrosion properties.

The thermal conductivity is lower than that for pure metals, and this is attributed to the lattice distortion effect. A presence of precipitates and a large amount of grain boundaries also lower the conductivity. The coefficient of thermal expansion for the studied HEA increases with temperature, and this to a higher degree than that of common superalloys, which may be a problem if they are to be joined together.

HEAs have been processed in different ways, but mainly via melting and casting. A certain scatter in properties has been noticed, and this is somewhat attributed to the presence of defects in the cast alloys, suggesting that these will need to be minimized if one wants to use HEAs in aero engines.

Although many exiting properties have been either shown or are expected, there is still a long way to go before this type of material can replace the nickel based superalloys currently in use. As discussed in Chapter 2, HEAs are not the only potential new materials type for aero engine usage, there are also CMCs and intermetallics, which may very well ”beat” HEAs. One of the advantages of HEAs is the fact that they are rather similar to superalloys, indicating that the processes used to create and shape the superalloys of today may very well be able to create and shape the HEAs of tomorrow. Providing that this is possible it will make HEAs the cheaper alternative since most of the needed structure is already in place.

5.2 Future Prospects in Aero Engine Parts

As previously mentioned HEAs are rather new, and their properties are not mapped enough for industrial use. Despite this the following section will try to suggest some systems for potential further studies regarding usage in the specific aero engine parts

discussed in section 2.4, based on what was learned in Chapter 2 and Chapter 3.

5.2.1 Structural Components

The limiting properties for the LCSs outlined in section 2.4 was primarily good *LCF* properties, followed by *strength*, *stiffness*, *creep/thermo mechanical fatigue* and good *oxidation* properties. Neither of these properties are particularly well-researched, and the proposed system will be based on rather vague terms.

It has been noted that the best fatigue properties of the researched systems was for the fcc-based system, with the other more complex system not far behind. As for creep, it has not been studied, but HEAs should generally have good creep resistance, and if not there is the possibility to coarsen the grains. On the other hand, a high strength can come from fine grains, solid solution strengthening and precipitation hardening. To increase the probability of good oxidation resistance aluminium and chromium have been suggested as valuable constituents in the system.

Building on this, a good candidate material for the LCS would have a single fcc phase to get good fatigue properties, with strengthening mainly by solid solution and (if the creep properties allow) nanoscale grains. It should contain both aluminium and chromium to increase the oxidation resistance. If the creep properties is not good enough with nanoscale grains some strength may perhaps be sacrificed for this by coarsening the grains.

Based on this, and what has been discussed in Chapter 3, Al-Co-Cr-Fe-Ni-Mo would be a potential candidate system. Preferably with a concentration of Al low enough to have only a fcc phase, as well as a low enough concentration of Mo so that the α phase will not form and the Mo-atoms will contribute to solid solution strengthening. It may be possible to have larger amounts of Mo before the α phase forms if the alloy is produced via MA instead of casting, increasing the homogeneity of the alloy. If the strength gained from solid solution strengthening and fine grain sizes is not enough, it might be possible to increase the Mo-content to allow for some α precipitates without sacrificing too much of the LCF properties.

Wanting a single disordered fcc phase, the phase determining parameters described in section 3.1.2 can be used to get an indication of which compositions will be viable. Figure 5.1 shows how δ, ΔS_{mix}, ΔH_{mix} and Ω varies with aluminium and molybdenum concentration in the $\text{Al}_x\text{CoCrFeNiMo}_z$ system. In Figure 5.1 it is seen that the parameter mist likely to be outside of the recommended values for whether a single disordered phase will be formed is the atomic size difference δ (which can be seen for the relevant elements in Table 5.1).

Another relevant parameter is the VEC, which gives an indication of which structure the formed phase will have, and Figure 5.2 shows how the VEC varies with aluminium and molybdenum concentration in the $\text{Al}_x\text{CoCrFeNiMo}_z$ system. As can be seen this will be the major limiting factor regarding the aluminium and molybdenum concentration, due to their low VEC, seen in Table 5.1. The empirical limit for fcc phase is $VEC \geq 8$ [42], and with aluminium and molybdenum both having values below this they will work towards a bcc phase. Adding elements with higher VEC or increasing the ratio of

Table 5.1: VEC, r and T_m for the elements in the suggested systems.

	Al	**Co**	**Cr**	**Fe**	**Ni**	**Mo**
VEC [36]	3	9	6	8	10	6
r (Å) [36]	1.432	1.251	1.249	1.241	1.246	1.363
T_m (K) [3]	933	1768	2148	1811	1726	2890

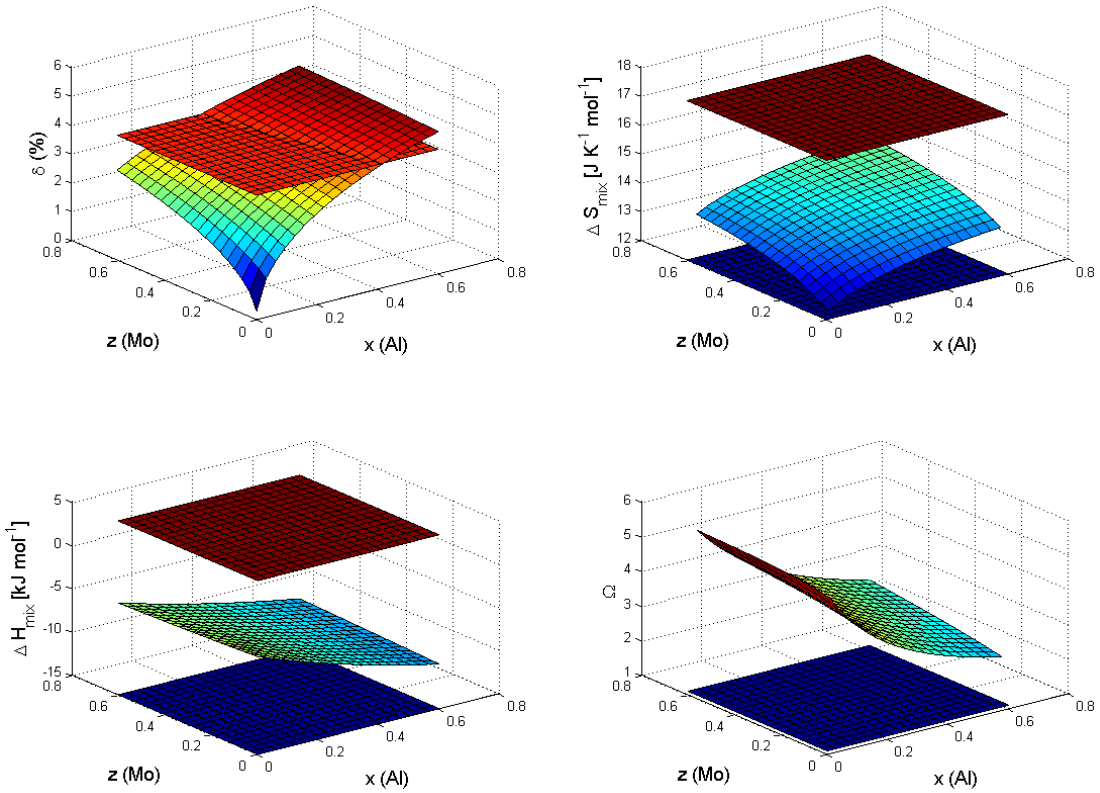

Figure 5.1: δ, ΔS_{mix}, ΔH_{mix} and Ω for $\text{Al}_x\text{CoCrFeNiMo}_z$. The constant planes are the limiting values for the parameters as described in section 3.1.2.

elements like nickel or cobalt which have high VEC might then stabilize the fcc phase, provided that they do not have too high/low enthalpies of mixing with the other elements and the atomic size do not differ by too much.

5.2.2 Heat Shields

The limiting properties for the heat shields outlined in section 2.4 were *temperature stability*, *formability* along with good *creep*,*LCF* and *oxidation properties*. Again, it is a bit vague how to achieve these properties, even though it is clearer than how to

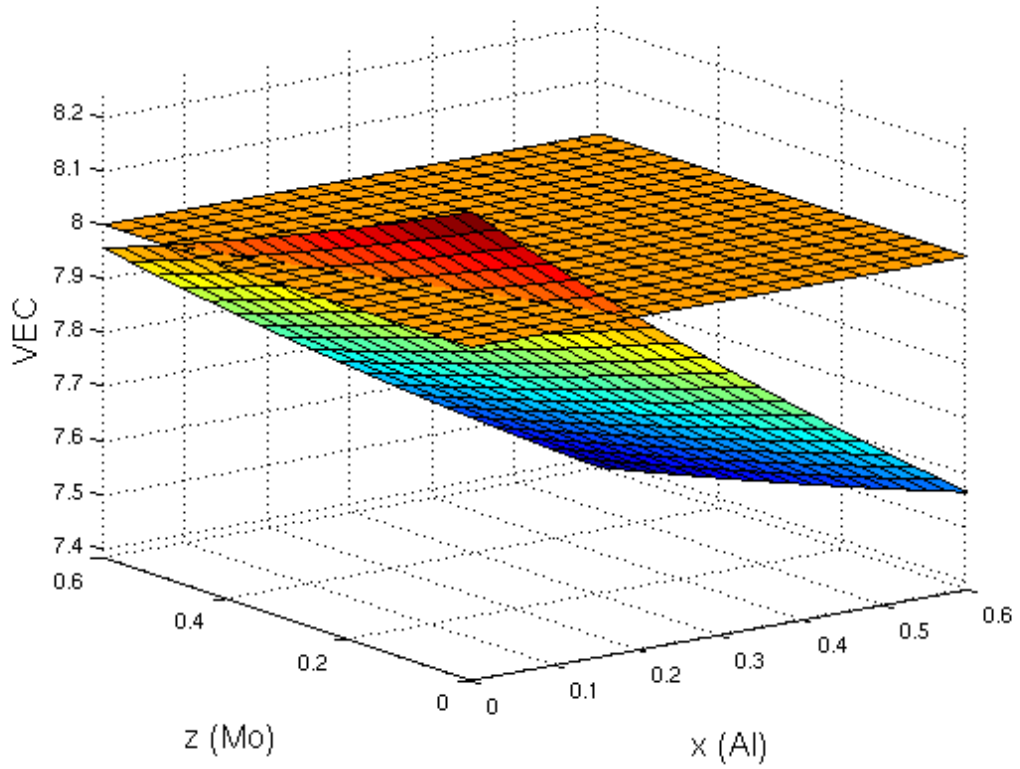

Figure 5.2: *VEC* for $Al_xCoCrFeNiMo_z$. The constant plane is the fcc limiting value for the VEC as described in section 3.1.2.

achieve those of the LCSs. How to achieve good thermal stability is still unclear, but conventionally there is a better chance for systems based on simple phases, whose main method of strengthening is solid solution strengthening.

The heat shield material should according to conventional knowledge be a single phase solid solution to get the best temperature stability. The creep resistance would benefit from coarse grains and the oxidation resistance would benefit from the inclusion of Al and Cr. If needed and if possible the thermal conductivity could be lowered by having finer grains, but the creep properties is prioritized. This could perhaps be achieved with the Al-Co-Cr-Fe-Ni system, with Al content low enough to have only the fcc phase. This system is also promising since it has been shown to be forgeable.

It should again be mentioned that many of these suggestions, in this and the previous section, are based on existing research which in no way are claimed to be extensive. The fatigue property is one such instance, where there has been a comparison between two alloys, one fcc structured and one bcc structured. The fcc structured alloy had slightly better properties, but not by much, and this is what the single fcc phase suggestion is based on. In the article there was not even just a single fcc phase, there were actually

two fcc phases, one of which was rich in Cu. The reason for disregarding this in the suggestions is that the variations of Al-Co-Cr-Cu-Fe-Ni-X without Cu have generally shown better properties than those with Cu.

If one can solve the issues mentioned in Chapter 4 for these suggested HEA systems, they might very well be good contenders for potential usage in future aero engines, lowering the weight of the engine which as previously discussed can lead to great gains to among other things the fuel efficiency.

5.2.3 Nozzle and Cone

The most important properties for the cone and nozzle in section 2.4 are *temperature stability*, *creep resistance* and *low density*. Again a single solid solution phase would be wanted for the thermal stability, with coarse grains for the creep resistance. To achieve as low density as possible, making it generally consist of light elements would also be good. It will be hard to compete with ceramics when it comes to density though. Perhaps some derivations of the low-density HEAs mentioned in section 3.3.1 can be used. In that case preferably the Al-Nb-Ti-V system since it already is a single phase coarse grained alloy with good temperature capability. The brittleness at room temperature will have to be solved, perhaps by either replacing an element or just adding a new fcc phase stabilizing element. The other low-density alloy, $Al_{20}Li_{20}Mg_{10}Sc_{20}Ti_{30}$, is also interesting due to its extremely low density, however as long as it contains such large amounts of Sc it is not really a feasible alternative. If the Sc could be replaced by another more common element and meanwhile the alloy can retain its properties, there are many potential applications.

Bibliography

[1] Y. Zhang, Y. Zhou, J. Lin, G. Chen, P. Liaw, Solid-Solution Phase Formation Rules for Multi-component Alloys, Advanced Engineering Materials 10 (6) (2008) 534–538.
URL http://dx.doi.org/10.1002/adem.200700240

[2] F. Campbell, Chapter 6 - superalloys, in: F. Campbell (Ed.), Manufacturing Technology for Aerospace Structural Materials, Elsevier Science, Oxford, 2006, pp. 211 – 272.
URL http://www.sciencedirect.com/science/article/pii/B9781856174954500068

[3] C. Nordling, J. Österman, Physics handbook for science and engineering, Studentlitteratur, Lund, 2006.

[4] F. Campbell, Chapter 2 - aluminum, in: F. Campbell (Ed.), Manufacturing Technology for Aerospace Structural Materials, Elsevier Science, Oxford, 2006, pp. 15 – 92.
URL http://www.sciencedirect.com/science/article/pii/B9781856174954500020

[5] A. Feuerstein, J. Knapp, T. Taylor, A. Ashary, A. Bolcavage, N. Hitchman, Technical and economical aspects of current thermal barrier coating systems for gas turbine engines by thermal spray and ebpvd: A review, Journal of Thermal Spray Technology 17 (2) (2008) 199–213.
URL http://dx.doi.org/10.1007/s11666-007-9148-y

[6] F. Campbell, Chapter 4 - titanium, in: F. Campbell (Ed.), Manufacturing Technology for Aerospace Structural Materials, Elsevier Science, Oxford, 2006, pp. 119 – 174.
URL http://www.sciencedirect.com/science/article/pii/B9781856174954500044

[7] R. Boyer, An overview on the use of titanium in the aerospace industry, Materials Science and Engineering: A 213 (1–2) (1996) 103 – 114, international Symposium on Metallurgy and Technology of Titanium Alloys.
URL http://www.sciencedirect.com/science/article/pii/0921509396102331

[8] J. C. Williams, E. A. S. Jr., Progress in structural materials for aerospace systems, Acta Materialia 51 (19) (2003) 5775 – 5799, the Golden Jubilee Issue. Selected topics in Materials Science and Engineering: Past, Present and Future.
URL http://www.sciencedirect.com/science/article/pii/S1359645403005020

[9] A. Materials, Titanium Alloys - Physical Properties (nov 2014).
URL http://www.azom.com/article.aspx?ArticleID=1341

[10] T. M. Pollock, S. Tin, Nickel-based superalloys for advanced turbine engines: chemistry, microstructure and properties, Journal of propulsion and power 22 (2) (2006) 361–374.
URL http://arc.aiaa.org/doi/abs/10.2514/1.18239

[11] R. Smallman, R. BiShop, Chapter 9 - modern alloy developments, in: R. Smallman, R. BiShop (Eds.), Modern Physical Metallurgy and Materials Engineering (Sixth edition), sixth edition Edition, Butterworth-Heinemann, Oxford, 1999, pp. 297 – 319.
URL http://www.sciencedirect.com/science/article/pii/B9780750645645500094

[12] R. W. Group, Turbine blade metallurgy (dec 2014).
URL http://www.rwgroup.com/index/turbine-blade-metallurgy

[13] R. E. Schafrik, D. D. Ward, J. R. Groh, Application of alloy 718 in ge aircraft engines: past, present and next five years, Superalloys 718, 625, 706 and various derivatives (2001) 1–11.
URL http://www.tms.org/superalloys/10.7449/2001/superalloys_2001_1_11.pdf

[14] N. R. Muktinutalapati, Materials for gas turbines–an overview, Advances in Gas Turbine Technology VIT University India.
URL http://cdn.intechopen.com/pdfs-wm/22905.pdf

[15] R. MacKay, T. Gabb, J. Smialek, M. Nathal, A new approach of designing superalloys for low density, JOM 62 (1) (2010) 48–54.
URL http://dx.doi.org/10.1007/s11837-010-0011-0

[16] P. Caron, T. Khan, Evolution of ni-based superalloys for single crystal gas turbine blade applications, Aerospace Science and Technology 3 (8) (1999) 513 – 523.

URL http://www.sciencedirect.com/science/article/pii/S127096389900108X

[17] H. Ohnabe, S. Masaki, M. Onozuka, K. Miyahara, T. Sasa, Potential application of ceramic matrix composites to aero-engine components, Composites Part A: Applied Science and Manufacturing 30 (4) (1999) 489 – 496.
URL http://www.sciencedirect.com/science/article/pii/S1359835X98001390

[18] R. Naslain, Design, preparation and properties of non-oxide CMCs for application in engines and nuclear reactors: an overview, Composites Science and Technology 64 (2) (2004) 155 – 170.
URL http://www.sciencedirect.com/science/article/pii/S0266353803002306

[19] A. Lasalmonie, Intermetallics: Why is it so difficult to introduce them in gas turbine engines?, Intermetallics 14 (10–11) (2006) 1123 – 1129, eUROMAT 2005 European Congress on Advanced Materials and Processes.
URL http://www.sciencedirect.com/science/article/pii/S0966979506000835

[20] G. Reports, This Electron Gun Builds Jet Engines (dec 2014).
URL http://www.gereports.com/post/94658699280/this-electron-gun-builds-jet-engines

[21] Materials Needs and Research and Development Strategy for Future Military Aerospace Propulsion Systems, The National Academies Press, 2011.
URL http://www.nap.edu/openbook.php?record_id=13144&page=189

[22] N. P. Padture, M. Gell, E. H. Jordan, Thermal barrier coatings for gas-turbine engine applications, Science 296 (5566) (2002) 280–4.
URL http://search.proquest.com/docview/213585327?accountid=10041

[23] A. Evans, D. Clarke, C. Levi, The influence of oxides on the performance of advanced gas turbines, Journal of the European Ceramic Society 28 (7) (2008) 1405 – 1419, developments in Ceramic Science and Engineering: the last 50 years. A meeting in celebration of Professor Sir Richard Brook's 70th Birthday.
URL http://www.sciencedirect.com/science/article/pii/S0955221907005948

[24] A. Maricocchi, A. Bartz, D. Wortman, Pvd tbc experience on ge aircraft engines, Journal of Thermal Spray Technology 6 (2) (1997) 193–198.
URL http://dx.doi.org/10.1007/s11666-997-0012-x

[25] I. Voutchkov, A. Keane, A. Bhaskar, T. M. Olsen, Weld sequence optimization: The use of surrogate models for solving sequential combinatorial problems, Computer Methods in Applied Mechanics and Engineering 194 (30–33) (2005)

3535 – 3551, structural and Design Optimization.
URL http://www.sciencedirect.com/science/article/pii/S0045782505000605

[26] A. W. International, Inconel 718 – composition, properties and applications of inconel 718 nickel-chromium alloy (dec 2014).
URL http://www.azom.com/article.aspx?ArticleID=4198

[27] H. International, Alloy at a glance haynes® waspaloy alloy (nov 2014).
URL http://www.haynesintl.com/pdf/h3128.pdf

[28] H. International, Haynes® 230® alloy information (nov 2014).
URL http://www.haynesintl.com/230HaynesAlloy.htm

[29] MatWEB, Special metals inconel alloy 718 (oct 2014).
URL http://www.matweb.com/search/datasheet.aspx?matguid=94950a2d209040a09b89952d45086134

[30] H. T. Metals, Inconel 718 technical data (nov 2014).
URL http://www.hightempmetals.com/techdata/hitempInconel718data.php

[31] B. Murty, J. Yeh, S. Ranganathan, Chapter 1 - a brief history of alloys and the birth of high-entropy alloys, in: B. M. Y. Ranganathan (Ed.), High Entropy Alloys, Butterworth-Heinemann, Boston, 2014, pp. 1 – 12.
URL http://www.sciencedirect.com/science/article/pii/B9780128002513000018

[32] J.-W. Yeh, S.-K. Chen, S.-J. Lin, J.-Y. Gan, T.-S. Chin, T.-T. Shun, C.-H. Tsau, S.-Y. Chang, Nanostructured High-Entropy Alloys with Multiple Principal Elements: Novel Alloy Design Concepts and Outcomes, Advanced Engineering Materials 6 (5) (2004) 299–303.
URL http://dx.doi.org/10.1002/adem.200300567

[33] D. B. Miracle, J. D. Miller, O. N. Senkov, C. Woodward, M. D. Uchic, J. Tiley, Exploration and development of high entropy alloys for structural applications, Entropy 16 (1) (2014) 494–525, date revised - 2014-09-01; Last updated - 2014-09-08.
URL http://search.proquest.com/docview/1559715460?accountid=10041

[34] F. Otto, Y. Yang, H. Bei, E. George, Relative effects of enthalpy and entropy on the phase stability of equiatomic high-entropy alloys, Acta Materialia 61 (7) (2013) 2628 – 2638.
URL http://www.sciencedirect.com/science/article/pii/S1359645413000694

[35] C. Kittel, P. McEuen, Introduction to solid state physics, Vol. 8, Wiley New York, 1976.

[36] S. Guo, C. Liu, Phase stability in high entropy alloys: Formation of solid-solution phase or amorphous phase, Progress in Natural Science: Materials International 21 (6) (2011) 433 – 446.
URL http://www.sciencedirect.com/science/article/pii/S100200711260080X

[37] B. Ren, Z. Liu, D. Li, L. Shi, B. Cai, M. Wang, Effect of elemental interaction on microstructure of CuCrFeNiMn high entropy alloy system, Journal of Alloys and Compounds 493 (1–2) (2010) 148 – 153.
URL http://www.sciencedirect.com/science/article/pii/S0925838809027571

[38] B. Cantor, Stable and metastable multicomponent alloys, Annales de Chimie: Science des Materiaux 32 (3) (2007) 245–256, cited By (since 1996)8.
URL http://www.scopus.com/inward/record.url?eid=2-s2.0-34249909751&partnerID=40&md5=b5fd1aa0e3fe9d9fd7d86778a6fa35fd

[39] M.-H. Tsai, J.-W. Yeh, High-Entropy Alloys: A Critical Review, Materials Research Letters 2 (3) (2014) 107–123.
URL http://dx.doi.org/10.1080/21663831.2014.912690

[40] A. Inoue, Stabilization of metallic supercooled liquid and bulk amorphous alloys, Acta Materialia 48 (1) (2000) 279 – 306.
URL http://www.sciencedirect.com/science/article/pii/S1359645499003006

[41] X. Yang, Y. Zhang, Prediction of high-entropy stabilized solid-solution in multi-component alloys, Materials Chemistry and Physics 132 (2–3) (2012) 233 – 238.
URL http://www.sciencedirect.com/science/article/pii/S0254058411009357

[42] S. Guo, C. Ng, J. Lu, C. T. Liu, Effect of valence electron concentration on stability of fcc or bcc phase in high entropy alloys, Journal of Applied Physics 109 (10).
URL http://scitation.aip.org/content/aip/journal/jap/109/10/10.1063/1.3587228

[43] K.-Y. Tsai, M.-H. Tsai, J.-W. Yeh, Sluggish diffusion in Co–Cr–Fe–Mn–Ni high-entropy alloys, Acta Materialia 61 (13) (2013) 4887 – 4897.
URL http://www.sciencedirect.com/science/article/pii/S1359645413003431

[44] C.-J. Tong, M.-R. Chen, J.-W. Yeh, S.-J. Lin, S.-K. Chen, T.-T. Shun, S.-Y. Chang, Mechanical performance of the $Al_xCoCrCuFeNi$ high-entropy alloy system with multiprincipal elements, Metallurgical and Materials Transactions A 36 (5) (2005) 1263–1271.
URL http://dx.doi.org/10.1007/s11661-005-0218-9

[45] L. Wen, H. Kou, J. Li, H. Chang, X. Xue, L. Zhou, Effect of aging temperature on microstructure and properties of AlCoCrCuFeNi high-entropy alloy, Intermetallics 17 (4) (2009) 266 – 269, sixth International Conference on Bulk Metallic Glasses (BMG VI).
URL http://www.sciencedirect.com/science/article/pii/S0966979508002549

[46] K. Zhang, Z. Fu, J. Zhang, J. Shi, W. Wang, H. Wang, Y. Wang, Q. Zhang, Annealing on the structure and properties evolution of the CoCrFeNiCuAl high-entropy alloy , Journal of Alloys and Compounds 502 (2) (2010) 295 – 299.
URL http://www.sciencedirect.com/science/article/pii/S0925838809024104

[47] A. Kuznetsov, D. Shaysultanov, N. Stepanov, G. Salishchev, O. Senkov, Tensile properties of an AlCrCuNiFeCo high-entropy alloy in as-cast and wrought conditions , Materials Science and Engineering: A 533 (0) (2012) 107 – 118.
URL http://www.sciencedirect.com/science/article/pii/S0921509311012846

[48] M. Ivchenko, V. Pushin, N. Wanderka, High-entropy equiatomic AlCrFeCoNiCu alloy: Hypotheses and experimental data, Technical Physics 59 (2) (2014) 211–223.
URL http://dx.doi.org/10.1134/S1063784214020108

[49] Y. Wang, B. Li, M. Ren, C. Yang, H. Fu, Microstructure and compressive properties of AlCrFeCoNi high entropy alloy , Materials Science and Engineering: A 491 (1–2) (2008) 154 – 158.
URL http://www.sciencedirect.com/science/article/pii/S0921509308001123

[50] W.-R. Wang, W.-L. Wang, S.-C. Wang, Y.-C. Tsai, C.-H. Lai, J.-W. Yeh, Effects of Al addition on the microstructure and mechanical property of Al_xCoCrFeNi high-entropy alloys, Intermetallics 26 (0) (2012) 44 – 51.
URL http://www.sciencedirect.com/science/article/pii/S096697951200088X

[51] Y. Lu, Y. Dong, S. Guo, L. Jiang, H. Kang, T. Wang, B. Wen, Z. Wang, J. Jie, Z. Cao, et al., A promising new class of high-temperature alloys: Eutectic high-entropy alloys, Scientific reports 4.
URL http://www.nature.com/srep/2014/140827/srep06200/full/srep06200.html

[52] Y. Zhou, Y. Zhang, F. Wang, Y. Wang, G. Chen, Effect of Cu addition on the microstructure and mechanical properties of AlCoCrFeNiTi_0.5 solid-solution alloy, Journal of Alloys and Compounds 466 (1–2) (2008) 201 – 204.
URL http://www.sciencedirect.com/science/article/pii/S0925838807022190

[53] F. Wang, Y. Zhang, G. Chen, Atomic packing efficiency and phase transition in a high entropy alloy, Journal of Alloys and Compounds 478 (1–2) (2009) 321 – 324.
URL http://www.sciencedirect.com/science/article/pii/S0925838808020203

[54] Y. J. Zhou, Y. Zhang, Y. L. Wang, G. L. Chen, Solid solution alloys of $AlCoCrFeNiTi_x$ with excellent room-temperature mechanical properties, Applied Physics Letters 90 (18) (2007) –.
URL http://scitation.aip.org/content/aip/journal/apl/90/18/10.1063/1.2734517

[55] K. Zhang, Z. Fu, J. Zhang, W. Wang, H. Wang, Y. Wang, Q. Zhang, J. Shi, Microstructure and mechanical properties of $CoCrFeNiTiAl_x$ high-entropy alloys, Materials Science and Engineering: A 508 (1–2) (2009) 214 – 219.
URL http://www.sciencedirect.com/science/article/pii/S0921509309000021

[56] F. Wang, Y. Zhang, Effect of Co addition on crystal structure and mechanical properties of $Ti_{0.5}CrFeNiAlCo$ high entropy alloy, Materials Science and Engineering: A 496 (1–2) (2008) 214 – 216.
URL http://www.sciencedirect.com/science/article/pii/S0921509308005467

[57] Y. Zhou, Y. Zhang, T. Kim, G. Chen, Microstructure characterizations and strengthening mechanism of multi-principal component $AlCoCrFeNiTi_{0.5}$ solid solution alloy with excellent mechanical properties, Materials Letters 62 (17–18) (2008) 2673 – 2676.
URL http://www.sciencedirect.com/science/article/pii/S0167577X08000396

[58] S.-T. Chen, W.-Y. Tang, Y.-F. Kuo, S.-Y. Chen, C.-H. Tsau, T.-T. Shun, J.-W. Yeh, Microstructure and properties of age-hardenable $Al_xCrFe_{1.5}MnNi_{0.5}$ alloys, Materials Science and Engineering: A 527 (21–22) (2010) 5818 – 5825.
URL http://www.sciencedirect.com/science/article/pii/S0921509310005769

[59] M.-H. Tsai, H. Yuan, G. Cheng, W. Xu, W. W. Jian, M.-H. Chuang, C.-C. Juan, A.-C. Yeh, S.-J. Lin, Y. Zhu, Significant hardening due to the formation of a sigma phase matrix in a high entropy alloy, Intermetallics 33 (0) (2013) 81 – 86.
URL http://www.sciencedirect.com/science/article/pii/S0966979512003755

[60] G. Salishchev, M. Tikhonovsky, D. Shaysultanov, N. Stepanov, A. Kuznetsov, I. Kolodiy, A. Tortika, O. Senkov, Effect of Mn and V on structure and mechanical properties of high-entropy alloys based on CoCrFeNi system , Journal of Alloys and Compounds 591 (0) (2014) 11 – 21.

URL http://www.sciencedirect.com/science/article/pii/S092583881303212X

[61] J. He, W. Liu, H. Wang, Y. Wu, X. Liu, T. Nieh, Z. Lu, Effects of Al addition on structural evolution and tensile properties of the FeCoNiCrMn high-entropy alloy system , Acta Materialia 62 (0) (2014) 105 – 113.
URL http://www.sciencedirect.com/science/article/pii/S1359645413007222

[62] F. Otto, A. Dlouhý, C. Somsen, H. Bei, G. Eggeler, E. George, The influences of temperature and microstructure on the tensile properties of a CoCrFeMnNi high-entropy alloy , Acta Materialia 61 (15) (2013) 5743 – 5755.
URL http://www.sciencedirect.com/science/article/pii/S1359645413004503

[63] J. Zhu, H. Zhang, H. Fu, A. Wang, H. Li, Z. Hu, Microstructures and compressive properties of multicomponent AlCoCrCuFeNiMo$_x$ alloys, Journal of Alloys and Compounds 497 (1–2) (2010) 52 – 56.
URL http://www.sciencedirect.com/science/article/pii/S0925838810005554

[64] J. Zhu, H. Fu, H. Zhang, A. Wang, H. Li, Z. Hu, Microstructures and compressive properties of multicomponent AlCoCrFeNiMo$_x$ alloys, Materials Science and Engineering: A 527 (26) (2010) 6975 – 6979.
URL http://www.sciencedirect.com/science/article/pii/S0921509310007665

[65] S. Ma, Y. Zhang, Effect of Nb addition on the microstructure and properties of AlCoCrFeNi high-entropy alloy , Materials Science and Engineering: A 532 (0) (2012) 480 – 486.
URL http://www.sciencedirect.com/science/article/pii/S0921509311012275

[66] J. Zhu, H. Fu, H. Zhang, A. Wang, H. Li, Z. Hu, Synthesis and properties of multiprincipal component AlCoCrFeNiSi$_x$ alloys, Materials Science and Engineering: A 527 (27–28) (2010) 7210 – 7214.
URL http://www.sciencedirect.com/science/article/pii/S0921509310007872

[67] O. Senkov, G. Wilks, J. Scott, D. Miracle, Mechanical properties of NbMoTaW and VNbMoTaW refractory high entropy alloys, Intermetallics 19 (5) (2011) 698 – 706.
URL http://www.sciencedirect.com/science/article/pii/S0966979511000185

[68] O. Senkov, G. Wilks, D. Miracle, C. Chuang, P. Liaw, Refractory high-entropy alloys, Intermetallics 18 (9) (2010) 1758 – 1765.

URL http://www.sciencedirect.com/science/article/pii/S0966979510002475

[69] O. Senkov, J. Scott, S. Senkova, D. Miracle, C. Woodward, Microstructure and room temperature properties of a high-entropy TaNbHfZrTi alloy, Journal of Alloys and Compounds 509 (20) (2011) 6043 – 6048.
URL http://www.sciencedirect.com/science/article/pii/S0925838811005536

[70] O. Senkov, J. Scott, S. Senkova, F. Meisenkothen, D. Miracle, C. Woodward, Microstructure and elevated temperature properties of a refractory TaNbHfZrTi alloy, Journal of Materials Science 47 (9) (2012) 4062–4074.
URL http://dx.doi.org/10.1007/s10853-012-6260-2

[71] O. Senkov, C. Woodward, Microstructure and properties of a refractory $NbCrMo_{0.5}Ta_{0.5}TiZr$ alloy, Materials Science and Engineering: A 529 (0) (2011) 311 – 320.
URL http://www.sciencedirect.com/science/article/pii/S0921509311009932

[72] O. Senkov, S. Senkova, C. Woodward, D. Miracle, Low-density, refractory multi-principal element alloys of the Cr–Nb–Ti–V–Zr system: Microstructure and phase analysis, Acta Materialia 61 (5) (2013) 1545 – 1557.
URL http://www.sciencedirect.com/science/article/pii/S1359645412008361

[73] O. Senkov, S. Senkova, D. Miracle, C. Woodward, Mechanical properties of low-density, refractory multi-principal element alloys of the Cr–Nb–Ti–V–Zr system, Materials Science and Engineering: A 565 (0) (2013) 51 – 62.
URL http://www.sciencedirect.com/science/article/pii/S0921509312016966

[74] O. Senkov, S. Senkova, C. Woodward, Effect of aluminum on the microstructure and properties of two refractory high-entropy alloys, Acta Materialia 68 (0) (2014) 214 – 228.
URL http://www.sciencedirect.com/science/article/pii/S1359645414000469

[75] O. Senkov, C. Woodward, D. Miracle, Microstructure and properties of aluminum-containing refractory high-entropy alloys, JOM (2014) 1–13.
URL http://dx.doi.org/10.1007/s11837-014-1066-0

[76] X. Yang, Y. Zhang, P. Liaw, Microstructure and compressive properties of $NbTiVTaAl_x$ high entropy alloys, Procedia Engineering 36 (0) (2012) 292 – 298, {IUMRS} International Conference in Asia 2011.
URL http://www.sciencedirect.com/science/article/pii/S1877705812015706

[77] Y. Wu, Y. Cai, T. Wang, J. Si, J. Zhu, Y. Wang, X. Hui, A refractory $Hf_{25}Nb_{25}Ti_{25}Zr_{25}$ high-entropy alloy with excellent structural stability and tensile properties, Materials Letters 130 (0) (2014) 277 – 280.
URL http://www.sciencedirect.com/science/article/pii/S0167577X1400946X

[78] E. Fazakas, V. Zadorozhnyy, L. Varga, A. Inoue, D. Louzguine-Luzgin, F. Tian, L. Vitos, Experimental and theoretical study of $Ti_{20}Zr_{20}Hf_{20}Nb_{20}X_{20}$ (X=V or Cr) refractory high-entropy alloys, International Journal of Refractory Metals and Hard Materials 47 (0) (2014) 131 – 138.
URL http://www.sciencedirect.com/science/article/pii/S0263436814001516

[79] Y. Zhou, Y. Zhang, Y. Wang, G. Chen, Microstructure and compressive properties of multicomponent $Al_x(TiVCrMnFeCoNiCu)_{100-x}$ high-entropy alloys, Materials Science and Engineering: A 454–455 (0) (2007) 260 – 265.
URL http://www.sciencedirect.com/science/article/pii/S0921509306024439

[80] N. Stepanov, D. Shaysultanov, G. Salishchev, M. Tikhonovsky, Structure and mechanical properties of a light-weight AlNbTiV high entropy alloy, Materials Letters 142 (0) (2015) 153 – 155.
URL http://www.sciencedirect.com/science/article/pii/S0167577X1402165X

[81] K. M. Youssef, A. J. Zaddach, C. Niu, D. L. Irving, C. C. Koch, A novel low-density, high-hardness, high-entropy alloy with close-packed single-phase nanocrystalline structures, Materials Research Letters 0 (0) (0) 1–5.
URL http://dx.doi.org/10.1080/21663831.2014.985855

[82] C.-Y. Hsu, C.-C. Juan, W.-R. Wang, T.-S. Sheu, J.-W. Yeh, S.-K. Chen, On the superior hot hardness and softening resistance of $AlCoCr_xFeMo_{0.5}Ni$ high-entropy alloys, Materials Science and Engineering: A 528 (10–11) (2011) 3581 – 3588.
URL http://www.sciencedirect.com/science/article/pii/S0921509311000943

[83] W.-R. Wang, W.-L. Wang, J.-W. Yeh, Phases, microstructure and mechanical properties of $Al_xCoCrFeNi$ high-entropy alloys at elevated temperatures, Journal of Alloys and Compounds 589 (0) (2014) 143 – 152.
URL http://www.sciencedirect.com/science/article/pii/S0925838813028144

[84] C.-W. Tsai, Y.-L. Chen, M.-H. Tsai, J.-W. Yeh, T.-T. Shun, S.-K. Chen, Deformation and annealing behaviors of high-entropy alloy $Al_{0.5}CoCrCuFeNi$, Journal of Alloys and Compounds 486 (1–2) (2009) 427 – 435.

URL http://www.sciencedirect.com/science/article/pii/S092583880901322X

[85] W.-H. Wu, C.-C. Yang, L. Yeh, et al., Industrial development of high-entropy alloys, in: Annales De Chimie-Science Des Materiaux, Vol. 31, Paris; New York: Masson, 1978-, 2006, p. 737.
URL http://www.researchgate.net/publication/245440486_Industrial_development_of_high-entropy_alloys/file/e0b49528f8fc29d271.pdf

[86] J. He, C. Zhu, D. Zhou, W. Liu, T. Nieh, Z. Lu, Steady state flow of the feconicrmn high entropy alloy at elevated temperatures, Intermetallics 55 (0) (2014) 9 – 14.
URL http://www.sciencedirect.com/science/article/pii/S0966979514001964

[87] J.-M. Wu, S.-J. Lin, J.-W. Yeh, S.-K. Chen, Y.-S. Huang, H.-C. Chen, Adhesive wear behavior of Al_xCoCrCuFeNi high-entropy alloys as a function of aluminum content, Wear 261 (5–6) (2006) 513 – 519.
URL http://www.sciencedirect.com/science/article/pii/S0043164805005144

[88] M.-R. Chen, S.-J. Lin, J.-W. Yeh, M.-H. Chuang, S.-K. Chen, Y.-S. Huang, Effect of vanadium addition on the microstructure, hardness, and wear resistance of $Al_{0.5}$CoCrCuFeNi high-entropy alloy, Metallurgical and Materials Transactions A 37 (5) (2006) 1363–1369.
URL http://dx.doi.org/10.1007/s11661-006-0081-3

[89] M.-H. Chuang, M.-H. Tsai, W.-R. Wang, S.-J. Lin, J.-W. Yeh, Microstructure and wear behavior of $Al_xCo_{1.5}CrFeNi_{1.5}Ti_y$ high-entropy alloys, Acta Materialia 59 (16) (2011) 6308 – 6317.
URL http://www.sciencedirect.com/science/article/pii/S1359645411004551

[90] C.-Y. Hsu, T.-S. Sheu, J.-W. Yeh, S.-K. Chen, Effect of iron content on wear behavior of AlCoCrFe$_x$Mo$_{0.5}$ni high-entropy alloys, Wear 268 (5–6) (2010) 653 – 659.
URL http://www.sciencedirect.com/science/article/pii/S0043164809005754

[91] M.-R. Chen, S.-J. Lin, J.-W. Yeh, S.-K. Chen, Y.-S. Huang, C.-P. Tu, Microstructure and Properties of $Al_{0.5}$CoCrCuFeNiTi$_x$ (x=0-2.0) high-entropy alloys, MATERIALS TRANSACTIONS 47 (5) (2006) 1395–1401.
URL https://www.jstage.jst.go.jp/article/matertrans/47/5/47_5_1395/_article

[92] M. Hemphill, T. Yuan, G. Wang, J. Yeh, C. Tsai, A. Chuang, P. Liaw, Fatigue behavior of $Al_{0.5}$CoCrCuFeNi high entropy alloys, Acta Materialia 60 (16) (2012)

5723 – 5734.
URL http://www.sciencedirect.com/science/article/pii/S1359645412004181

[93] M. A. Hemphill, Fatigue behavior of high-entropy alloys, Master's thesis, University of Tennessee (2012).
URL http://trace.tennessee.edu/utk_gradthes/1383/

[94] Y. Chen, T. Duval, U. Hung, J. Yeh, H. Shih, Microstructure and electrochemical properties of high entropy alloys—a comparison with type-304 stainless steel, Corrosion Science 47 (9) (2005) 2257 – 2279.
URL http://www.sciencedirect.com/science/article/pii/S0010938X04003567

[95] Y. Chen, U. Hong, H. Shih, J. Yeh, T. Duval, Electrochemical kinetics of the high entropy alloys in aqueous environments—a comparison with type 304 stainless steel, Corrosion Science 47 (11) (2005) 2679 – 2699.
URL http://www.sciencedirect.com/science/article/pii/S0010938X04003439

[96] Y.-J. Hsu, W.-C. Chiang, J.-K. Wu, Corrosion behavior of FeCoNiCrCu$_x$ high-entropy alloys in 3.5% sodium chloride solution, Materials Chemistry and Physics 92 (1) (2005) 112 – 117.
URL http://www.sciencedirect.com/science/article/pii/S0254058405000088

[97] C. Lee, C. Chang, Y. Chen, J. Yeh, H. Shih, Effect of the aluminium content of $Al_xCrFe_{1.5}MnNi_{0.5}$ high-entropy alloys on the corrosion behaviour in aqueous environments, Corrosion Science 50 (7) (2008) 2053 – 2060.
URL http://www.sciencedirect.com/science/article/pii/S0010938X08001376

[98] C.-M. Lin, H.-L. Tsai, Evolution of microstructure, hardness, and corrosion properties of high-entropy $Al_{0.5}$CoCrFeNi alloy, Intermetallics 19 (3) (2011) 288 – 294.
URL http://www.sciencedirect.com/science/article/pii/S0966979510004243

[99] C.-M. Lin, H.-L. Tsai, H.-Y. Bor, Effect of aging treatment on microstructure and properties of high-entropy $Cu_{0.5}$CoCrFeNi alloy, Intermetallics 18 (6) (2010) 1244 – 1250.
URL http://www.sciencedirect.com/science/article/pii/S096697951000172X

[100] C. Lee, Y. Chen, C. Hsu, J. Yeh, H. Shih, The Effect of Boron on the Corrosion Resistance of the High Entropy Alloys $Al_{0.5}$CoCrCuFeNiB$_x$, Journal of the Elec-

trochemical Society 154 (8) (2007) C424–C430.
URL http://jes.ecsdl.org/content/154/8/C424.full

[101] Y. Chou, J. Yeh, H. Shih, The effect of molybdenum on the corrosion behaviour of the high-entropy alloys $Co_{1.5}CrFeNi_{1.5}Ti_{0.5}Mo_x$ in aqueous environments, Corrosion Science 52 (8) (2010) 2571 – 2581.
URL http://www.sciencedirect.com/science/article/pii/S0010938X10001897

[102] C. Lee, Y. Chen, C. Hsu, J. Yeh, H. Shih, Enhancing pitting corrosion resistance of $Al_xCrFe_{1.5}MnNi_{0.5}$ high-entropy alloys by anodic treatment in sulfuric acid, Thin Solid Films 517 (3) (2008) 1301 – 1305, 35th International Conference on Metallurgical Coatings and Thin Films (ICMCTF).
URL http://www.sciencedirect.com/science/article/pii/S0040609008006500

[103] Y.-F. Kao, T.-D. Lee, S.-K. Chen, Y.-S. Chang, Electrochemical passive properties of $Al_xCoCrFeNi$ (x=0, 0.25, 0.50, 1.00) alloys in sulfuric acids, Corrosion Science 52 (3) (2010) 1026 – 1034.
URL http://www.sciencedirect.com/science/article/pii/S0010938X09005824

[104] Y. Chou, Y. Wang, J. Yeh, H. Shih, Pitting corrosion of the high-entropy alloy $Co_{1.5}CrFeNi_{1.5}Ti_{0.5}Mo_{0.1}$ in chloride-containing sulphate solutions, Corrosion Science 52 (10) (2010) 3481 – 3491.
URL http://www.sciencedirect.com/science/article/pii/S0010938X1000332X

[105] B. Ren, Z. X. Liu, D. M. Li, L. Shi, B. Cai, M. X. Wang, Corrosion behavior of CuCrFeNiMn high entropy alloy system in 1 M sulfuric acid solution, Materials and Corrosion 63 (9) (2012) 828–834.
URL http://dx.doi.org/10.1002/maco.201106072

[106] Z. Tang, L. Huang, W. He, P. K. Liaw, Alloying and processing effects on the aqueous corrosion behavior of high-entropy alloys, Entropy 16 (2) (2014) 895–911, copyright - Copyright MDPI AG 2014; Last updated - 2014-07-26.
URL http://search.proquest.com/docview/1537859077?accountid=10041

[107] C. Huang, Y. Zhang, J. Shen, R. Vilar, Thermal stability and oxidation resistance of laser clad TiVCrAlSi high entropy alloy coatings on Ti–6Al–4V alloy , Surface and Coatings Technology 206 (6) (2011) 1389 – 1395.
URL http://www.sciencedirect.com/science/article/pii/S0257897211008735

[108] A. D. Pogrebnjak, Structure and properties of nanostructured (ti-hf-zr-v-nb) n coatings, Journal of Nanomaterials 2013 (2013) 5.
URL http://www.hindawi.com/journals/jnm/2013/780125/

[109] O. Senkov, S. Senkova, D. Dimiduk, C. Woodward, D. Miracle, Oxidation behavior of a refractory $NbCrMo_{0.5}Ta_{0.5}TiZr$ alloy, Journal of Materials Science 47 (18) (2012) 6522–6534.
URL http://dx.doi.org/10.1007/s10853-012-6582-0

[110] M.-H. Hsieh, M.-H. Tsai, W.-J. Shen, J.-W. Yeh, Structure and properties of two Al–Cr–Nb–Si–Ti high-entropy nitride coatings, Surface and Coatings Technology 221 (0) (2013) 118 – 123.
URL http://www.sciencedirect.com/science/article/pii/S0257897213001138

[111] C. Liu, H. Wang, S. Zhang, H. Tang, A. Zhang, Microstructure and oxidation behavior of new refractory high entropy alloys, Journal of Alloys and Compounds 583 (0) (2014) 162 – 169.
URL http://www.sciencedirect.com/science/article/pii/S0925838813019634

[112] J. C. Jiang, X. Y. Luo, High temperature oxidation behaviour of AlCuTiFeNiCr high-entropy alloy, Advanced Materials Research 652 (2013) 1115–1118.
URL http://www.scientific.net/AMR.652-654.1115

[113] H.-P. Chou, Y.-S. Chang, S.-K. Chen, J.-W. Yeh, Microstructure, thermophysical and electrical properties in $Al_xCoCrFeNi$ ($0 \leq x \leq 2$) high-entropy alloys, Materials Science and Engineering: B 163 (3) (2009) 184 – 189.
URL http://www.sciencedirect.com/science/article/pii/S0921510709002438

[114] C.-L. Lu, S.-Y. Lu, J.-W. Yeh, W.-K. Hsu, Thermal expansion and enhanced heat transfer in high-entropy alloys, Journal of Applied Crystallography 46 (3) (2013) 736–739.
URL http://dx.doi.org/10.1107/S0021889813005785

[115] Y.-F. Kao, S.-K. Chen, T.-J. Chen, P.-C. Chu, J.-W. Yeh, S.-J. Lin, Electrical, magnetic, and Hall properties of $Al_xCoCrFeNi$ high-entropy alloys, Journal of Alloys and Compounds 509 (5) (2011) 1607 – 1614.
URL http://www.sciencedirect.com/science/article/pii/S0925838810027490

[116] S. Singh, N. Wanderka, K. Kiefer, K. Siemensmeyer, J. Banhart, Effect of decomposition of the Cr–Fe–Co rich phase of AlCoCrCuFeNi high entropy alloy on magnetic properties, Ultramicroscopy 111 (6) (2011) 619 – 622, special Issue: 52nd International Field Emission Symposium.
URL http://www.sciencedirect.com/science/article/pii/S0304399110003335

[117] X. Qiu, Y. Zhang, C. Liu, Effect of ti content on structure and properties of $Al_2CrFeNiCoCuTi_x$ high-entropy alloy coatings, Journal of Alloys and Compounds

585 (0) (2014) 282 – 286.
URL http://www.sciencedirect.com/science/article/pii/S0925838813022342

[118] N. Tariq, M. Naeem, B. Hasan, J. Akhter, M. Siddique, Effect of W and Zr on structural, thermal and magnetic properties of AlCoCrCuFeNi high entropy alloy, Journal of Alloys and Compounds 556 (0) (2013) 79 – 85.
URL http://www.sciencedirect.com/science/article/pii/S0925838812023195

[119] Y. Zhang, T. Zuo, Y. Cheng, P. K. Liaw, High-entropy alloys with high saturation magnetization, electrical resistivity, and malleability, Scientific reports 3.
URL http://www.ncbi.nlm.nih.gov/pmc/articles/PMC3598001/

[120] M. S. Lucas, L. Mauger, J. A. Muñoz, Y. Xiao, A. O. Sheets, S. L. Semiatin, J. Horwath, Z. Turgut, Magnetic and vibrational properties of high-entropy alloys, Journal of Applied Physics 109 (7).

[121] H. Zhang, Y. Pan, Y. He, H. Jiao, Microstructure and properties of 6FeNiCoSiCrAlTi high-entropy alloy coating prepared by laser cladding, Applied Surface Science 257 (6) (2011) 2259 – 2263.
URL http://www.sciencedirect.com/science/article/pii/S016943321001319X

[122] T.-t. Zuo, S.-b. Ren, P. Liaw, Y. Zhang, Processing effects on the magnetic and mechanical properties of $FeCoNiAl_{0.2}Si_{0.2}$ high entropy alloy, International Journal of Minerals, Metallurgy, and Materials 20 (6) (2013) 549–555.
URL http://dx.doi.org/10.1007/s12613-013-0764-x

[123] P. Koželj, S. Vrtnik, A. Jelen, S. Jazbec, Z. Jagličić, S. Maiti, M. Feuerbacher, W. Steurer, J. Dolinšek, Discovery of a superconducting high-entropy alloy, Phys. Rev. Lett. 113 (2014) 107001.
URL http://link.aps.org/doi/10.1103/PhysRevLett.113.107001

[124] K. Zhang, Z. Fu, Effects of annealing treatment on properties of $CoCrFeNiTiAl_x$ multi-component alloys, Intermetallics 28 (0) (2012) 34 – 39.
URL http://www.sciencedirect.com/science/article/pii/S0966979512001689

[125] B. Murty, J. Yeh, S. Ranganathan, Chapter 5 - Synthesis and Processing , in: B. M. Y. Ranganathan (Ed.), High Entropy Alloys, Butterworth-Heinemann, Boston, 2014, pp. 77 – 89.
URL http://www.sciencedirect.com/science/article/pii/B9780128002513000055

[126] F. Wang, Y. Zhang, G. Chen, H. Davies, Cooling rate and size effect on the microstructure and mechanical properties of AlCoCrFeNi high entropy alloy,

Journal of Engineering Materials and Technology 131 (3) (2009) 034501.
URL http://materialstechnology.asmedigitalcollection.asme.org/article.aspx?articleid=1428493

[127] S. Singh, N. Wanderka, B. Murty, U. Glatzel, J. Banhart, Decomposition in multi-component AlCoCrCuFeNi high-entropy alloy, Acta Materialia 59 (1) (2011) 182 – 190.
URL http://www.sciencedirect.com/science/article/pii/S1359645410005884

[128] Y. Zhang, S. Ma, J. Qiao, Morphology transition from dendrites to equiaxed grains for AlCoCrFeNi high-entropy alloys by copper mold casting and Bridgman solidification, Metallurgical and Materials Transactions A 43 (8) (2012) 2625–2630.
URL http://link.springer.com/article/10.1007/s11661-011-0981-8/fulltext.html

[129] V. Hammond, M. Atwater, K. Darling, H. Nguyen, L. Kecskes, Equal-channel angular extrusion of a low-density high-entropy alloy produced by high-energy cryogenic mechanical alloying, JOM 66 (10) (2014) 2021–2029.
URL http://dx.doi.org/10.1007/s11837-014-1113-x

[130] Y. Brif, M. Thomas, I. Todd, The use of high-entropy alloys in additive manufacturing, Scripta Materialia (0) (2014) –.
URL http://www.sciencedirect.com/science/article/pii/S1359646214005107

[131] MatWEB, TIMET 6-4 Titanium Alloy (Ti-6Al-4V; ASTM Grade 5) Sheet and Plate, 0.025-1.000 in, Annealed, Per ASTM B265 (oct 2014).
URL http://www.matweb.com/search/datasheet.aspx?matguid=a1fc12bc5d04434a8e617a745f46624b

[132] G. Welsch, R. Boyer, E. Collings, Materials Properties Handbook: Titanium Alloys, Materials properties handbook, ASM International, 1993.
URL https://books.google.se/books?id=x3rToHWOcD8C

[133] Veridiam, Titanium Alloy Ti 6Al-4V (jan 2015).
URL http://www.veridiam.com/pdf/DataSheetTitaniumAlloy.pdf